COMPREHENSIVE ELECTRICAL EVALUATION OF POLYALPHAOLEFIN (PAO) DIELECTRIC COOLANT

FINAL REPORT

SBIR CONTRACT N68335-97-C-0025

November 12, 1997

BELTRAN, INC
1133 East 35 Street
Brooklyn, NY 11210

Jacob Khodorkovsky
Boris Khusid
Andreas Acrivos
Michael Beltran

Prepared for

Naval Air Warfare Center - Aircraft Division
Patuxent River, MD 20670

REPORT DOCUMENTATION PAGE

Form Approved
OMB No. 0704-0188

1. AGENCY USE ONLY (Leave blank)	2. REPORT DATE	3. REPORT TYPE AND DATES COVERED
	12 Nov 97	Final - 17 Dec 96 - 1 Oct 97

4. TITLE AND SUBTITLE

Comprehensive Electrical Evaluation of Polyalphaolefin (PAO) Dielectric Coolant

5. FUNDING NUMBERS

N68335-97-C-0025

6. AUTHOR(S)

Jacob Khodorkovsky, Boris Khusid, Andreas Acrivos, Michael Beltran

7. PERFORMING ORGANIZATION NAME(S) AND ADDRESS(ES)

Beltran, Inc.
1133 East 35 Street
Brooklyn, NY 11210

8. PERFORMING ORGANIZATION REPORT NUMBER

9. SPONSORING/MONITORING AGENCY NAME(S) AND ADDRESS(ES)

Naval Air Warfare Center
Aircraft Division
Patuxent River, MD 20670

10. SPONSORING/MONITORING AGENCY REPORT NUMBER

11. SUPPLEMENTARY NOTES

12a. DISTRIBUTION/AVAILABILITY STATEMENT

Approved for public release; distribution is unlimited.

12b. DISTRIBUTION CODE

A

13. ABSTRACT (Maximum 200 words)

We found that

- Electrical breakdown in a PAO fluid results in the formation of submicron carbonaceous particles and some flammable gas which, more than likely, is hydrogen.
- An applied electric field generates significant streaming electrification in a PAO fluid.
- The Navy Oil Analysis Program procedures, which were developed in the 1980s for testing hydrolytically unstable Coolanol fluids, fail to test the degradation of hydrolytically stable PAO fluids currently used by the Navy.
- All the following measurements of: 1) the frequency dependence of a complex dielectric permittivity (dielectric spectrum); 2) the partial discharge inception voltage using needle-plane electrodes; 3) the viscosity in a thin capillary; and 4) the transmittance in ultra-violet and visible light, appear to be sensitive enough to characterize the PAO fluid degradation under operating conditions typical of Navy aircraft systems. Moreover, these test procedures are simpler, faster, and less expensive than those currently being employed at the Navy laboratories.

14. SUBJECT TERMS	15. NUMBER OF PAGES
Polyalphaolefin, Dielectric Coolant, Electrification, Aggregation, Dielectrophoresis, Electro-separation, Heat transfer	46
	16. PRICE CODE

17. SECURITY CLASSIFICATION OF REPORT	18. SECURITY CLASSIFICATION OF THIS PAGE	19. SECURITY CLASSIFICATION OF ABSTRACT	20. LIMITATION OF ABSTRACT
Unclassified	Unclassified	Unclassified	UL

EXECUTIVE SUMMARY

We found that

- Electrical breakdown in a PAO fluid results in the formation of submicron carbonaceous particles and some flammable gas which, more than likely, is hydrogen.
- An applied electric field generates significant streaming electrification in a PAO fluid.
- The Navy Oil Analysis Program procedures, which were developed in the 1980s for testing hydrolytically unstable Coolanol fluids, fail to test the degradation of hydrolytically stable PAO fluids currently used by the Navy.
- All the following measurements of:

  1) the frequency dependence of a complex dielectric permittivity (dielectric spectrum);
  2) the partial discharge inception voltage using needle-plane electrodes;
  3) the viscosity in a thin capillary; and
  4) the transmittance in ultra-violet and visible light,

  appear to be sensitive enough to characterize the PAO fluid degradation under operating conditions typical of Navy aircraft systems. Moreover, these test procedures are simpler, faster, and less expensive than those currently being employed at the Navy laboratories.

We developed a novel electro-separation technique and substantiated its ability to remove contaminants from a PAO fluid.

Our studies indicate that the development of an instrumentation and technique for the condition-based monitoring of in-use PAO fluids and their remediation should significantly improve the effectiveness and reduce the procurement and maintenance costs of aircraft systems.

TABLE OF CONTENTS

LIST OF FIGURES

1. BACKGROUND OF DIELECTRIC COOLANTS USED IN AIRCRAFT SYSTEMS

A new radar coolant has been introduced but the test method did not change.
A new test method or procedure is needed, as proposed.

Selecting a dielectric fluid to be used for both cooling and electrical insulation of a power system equipment at high temperatures and high electric stresses is a complex task, based on a number of interrelated and technical considerations. For example, flowing dielectric fluids very often lead to failures of electrical equipment since a flow causes the transport and accumulation of charges that can create electric fields which can exceed the electrical breakdown strength of the materials in the equipment. Although the price per gallon of each fluid is important, the actual cost of operation, including capital, operating, and maintenance costs, will be determined by many other factors. That is why the electric-field-induced phenomena in flowing dielectric fluids and their degradation under high mechanical, temperature, and electrical stresses have been investigated extensively for decades by many researchers all over the world.

References [1, 2] highlight the problems associated with the use of silicate-ester-based dielectric coolants (Coolanol) in radar coolant applications in US Navy aircraft weapon and ground support systems. Hardware failures resulted from the decomposition of the silicate-ester-based fluids in the presence of moisture and high electrical stresses, which led to the formation of silica gels that, in turn, formed deposits on the electrical components. This process also formed a highly flammable alcohol by-product which reduced the flash point of the coolant fluid. After the loss of a US Navy aircraft in 1978 attributed to a silicate-ester-based fluid fire, an effort was initiated to find a viable solution to these problems. Field investigations confirmed that when certain avionics were opened for inspection, seventy percent were found to be grossly contaminated with a particulate matter generated from silicate-ester-based fluid degradation [2]. A "black plague", which referred to the formation of black and gray particles, was found on electrical circuit boards and at high voltage connections of radar transmitters. Some of the units contained evidence of massive arcing and case damage.

After an extensive screening of candidate fluids by the Navy and the Air Force laboratories, a hydrogenated polyalphaolefin-based (PAO) fluid emerged as the best replacement candidate. The PAO fluid properties are equal to or better than the Navy radar coolant property requirements and offer a significant improvement in hydrolytic stability, hygroscopic tendency, and lubricity over the silicate-ester-based fluids [3]. Compared to conventional mineral oils and many synthetic lubricants, PAO-based fluids exhibit low volatility and pour points, high flash points (from 222°C to 268°C) and fire points (from 248°C to 298°C), and excellent thermal and oxidation stability. Their high viscosity indices insure minimal viscosity changes with fluctuations in temperature and permit the formulation of full synthetic motor oils without viscosity index improvers [4].

To date, the Navy has converted several of its aircraft weapon and ground support equipment to PAO fluids. A fluid specification which covers the PAO fluid properties, MIL-C-87252B [3], has been issued and widely distributed throughout the industry and the services.

Presently, a number of different commercial suppliers provide fluids conforming to the MIL-C-87252B specification.

The procedures currently employed at Navy laboratories for routine testing of fluid samples which originated from avionic cooling systems were developed about 10-15 years ago to test the extent of hydrolysis of Coolanol. These testing techniques, specified by the Navy Oil Analysis Program (NOAP), are listed in Table 1.

TABLE 1. PROCEDURES USED IN NAVY LABORATORIES

Characteristics	Test Methods
Water Content	ASTM 1744-92, ASTM D 1533-88 (B)
Specific Resistivity	ASTM D 1169-89, ASTM D 257-93
Dielectric Strength	ASTM D 1816-84A, ASTM D 877-87
Flash Point	ASTM D 92
Particle (> 5 μm) Contamination	Navy Standard For Particle Contamination

These procedures are "a go, no-go test". The fluid is declared good or bad depending on the outcome of this test. Since the 80's this extensive and costly fluid monitoring has remained intact, even though the Navy aircraft systems have been converted to PAO fluids. However, a correlation of the fluid sample failures with aircraft hardware failures has not been demonstrated. What this means is that these routine procedures fail to test the extent of the decomposition of PAO fluids. Moreover, we found that no reliable data exist concerning the influence of operating conditions in aircraft systems on PAO fluid degradation. As a result, the use of currently available testing procedures leads to an unreasonably shortened fluid lifetime in aircraft systems and, in turn, to excessive manpower losses. This indicates that different procedures should be employed for the testing of PAO fluid samples.

In order to specify when a PAO fluid in aircraft forced-cooled high-voltage electrical equipment should be changed, one needs test procedures that enable one to determine the extent of the decomposition of the sampled fluid and its ability to withstand high voltage. The potential benefits of such test procedures, which we plan to develop, are associated with the fast growth of the use of PAO-based fluids in electrical equipment for industrial and military applications.

2. ACCOMPLISHMENTS UNDER THE NAVY PHASE I SBIR PROGRAM SUPPORT

Parameters that account for radar coolant degradation have been identified in laboratory simulated test rigs.

2.1. Efforts

2.1.1. Effects of mechanical, temperature, and electrical stresses on the service properties of hydrocarbon fluids

Since there are no reliable data on PAO fluid degradation under operating conditions in Navy aircraft systems, we analyzed the state-of-the-art [5-9] of the electric-thermal-mechanical aging of low-conducting hydrocarbon fluids (specifically, PAO fluids are in this category). We shall summarize below the main variables that influence the decomposition of hydrocarbon fluids. It appears reasonable to suggest that these variables will be important in the case of Navy aircraft systems as well.

As found in recent theoretical and experimental studies [5-9], two important factors impact the degradation of service properties of a flowing hydrocarbon fluid. First, the charges that are generated by streaming electrification can accumulate in some parts of the hydraulic circuit and thereby significantly increase the electric field in these regions. Moreover, the fluid motion alters the dielectric strength of the fluid in a complex manner. Both these aspects need to be understood to permit the design, operation, and monitoring of forced-cooled electrical equipment.

Velocity

There is universal agreement that the flow rate of dielectric fluid is one of the primary driving factors in electrification [6-9]. The motion of a fluid is important for a number of reasons [9-11]. First, appreciable fluid velocities change the effective mobility of an ion, since ions not only drift in the field but are also convected in the field direction by a component of the fluid motion. Second, the fluid motion can have a significant impact on the electrical breakdown of an electrically stressed fluid since local low-pressure zones at the centers of strong vortices generate nucleation points for the breakdown, thereby decreasing the overall dielectric strength. Third, any abrupt changes in the flow geometry due to the presence of spacers can create cavitation, thus reducing the electric strength of composite insulation structures. Finally, the charge carried by the flow can also create field distortions in the gap. This space charge field intensification is of particular interest at present since a number of anomalous power equipment failures have been linked to electrokinetic effects in flowing dielectric fluids [6-9].

Temperature

Temperature affects almost all the hydrodynamic, electrical, and chemical fluid properties in complex ways and, thus, the charge densities generated in a circulating fluid are dependent on the operating conditions [6-9]. For example, the thermal stability of an organic fluid is a function of the fluid's chemistry, the temperature to which it is exposed, and the duration of the exposure. Over time, at a given temperature, the fluid will begin to degrade. Degradation usually produces "low boilers" (also known as non-condensables) having boiling points lower than the remaining fluid, and "high boilers", having higher boiling points than the fluid [12]. Although low boilers are vented from the system, high boilers remain in the fluid, and their concentration determines when the fluid has reached the end of its useful life. The rate at which this breakdown occurs is called the degradation rate and is a very strong function of temperature, typically following an Arrhenius type of relationship. A general rule with organic fluids is that the degradation rate doubles for every 18 - 21°F increase in the fluid temperature [12].

Moisture content

Water is a polar molecule that is a known contaminant in most hydrocarbon fluids. At very low levels below several ppm, there exists good evidence that the charge generation increases with moisture, presumably as a result of the availability of ions. It is likely that the predominant effect of moisture content at higher levels is through the change it brings about in the conductivity of the fluid which impacts the dielectric relaxation phenomena [9].

Contaminants

The effect of trace contaminants (particulates and gas bubbles) on the flow electrification and electrical breakdown processes extends to self-contamination due to the aging of the fluid, the leaching of ionic species from solid constructional materials, and the creation of gas and vapor bubbles and carbon particles by repeated discharges and the heating of the fluid up to temperatures close to its flash point [6-9, 12]. These particulates and bubbles can be transported by the fluid to the region between the high and low voltage windings. A local surface charge can also give rise to electrostatic precipitator action and attract fluid-borne bubbles and particulates into high electric field regions [13]. If enough bubbles or particulates accumulate due to re-circulatory flow, the dielectric strength of the insulating fluid is sufficiently reduced with the consequent possibility of triggering an electrical breakdown [13, 14].

Charge accumulation

Ionic charges resulting from dissociable impurities in the dielectric fluid form a weakly-bound double-layer at solid interfaces containing ions that can be stripped and transported downstream by the fluid motion [9, 15-17]. The resulting charge separation at interfaces between a moving fluid and a solid boundary can give rise to the generation of substantial electric fields which, either alone or in concert with the existing electric fields imposed by the energization of the equipment, can lead to a failure of the insulation. Recent power equipment failures point to surface charges as the primary cause.

Numerous attempts have been made to develop a procedure for measuring the charge density in a flowing dielectric fluid which can be applied in an industrial environment [9, 18-20]. Traditional instruments rely on measuring the charge relaxation in a sampled fluid but require an inconveniently large chamber to insure that dielectric relaxation is complete. In addition, such a technique cannot differentiate with high accuracy the effects of flow electrification through the instrument from the desired charge density to be measured. To avoid these limitations, a tandem-chamber monitor [18] and an absolute charge sensor [19, 20] have been developed which unambiguously measure the local charge density in a flowing fluid.

Superimposed electric stress

The application of an external electric field of the order of one kV/mm to a flowing fluid intensifies the charge generation process at solid interfaces [5-8]. This causes the streaming current to increase with the strength of the applied AC field [21]. The relation between the streaming current and the strength of the applied DC field is more complicated and, in addition, depends essentially on the polarity of the field [21]. The enhancement factors to account for the influence of the strength of the applied electric field on the streaming current generally vary between 2 and 8 depending on the structure of the flow-assembly and other variables [9].

Dielectric integrity of moving fluids

The fluid motion produces a modest (about 15%) improvement in the mean breakdown voltage of the fluid and results in a significant change in the statistics of the fluid electrical breakdown. Specifically, the fluid flow eliminates the negative skew and the long tail of the probability distribution function of the number of discharges in the low-voltage region which, in turn, generates a significant (about 50%) improvement in the apparent fluid breakdown strength at the, say, 1% probability level [9-11]. The explanation proposed is that the flow of the fluid prevents the establishment of particle chains bridging the gap and sweeps any bubbles that might facilitate electrical breakdown.

2.1.2. Plausible mechanisms of PAO fluid degradation and weaknesses of the test procedures currently employed by the Navy laboratories

To study the NOAP sampling and testing procedures and available experimental data on the PAO fluid degradation, Dr. Khusid visited The Mid-Atlantic Regional Calibration & Materials Test Laboratories, NARF Norfolk, VA, and The Materials Engineering Laboratory, Naval Air Depot, North Island, San Diego, CA. These visits were arranged by Dr. Suresh Verma, the Navy manager of this project. Technical discussions in these Laboratories were held with Mr. Bill Zdrojewski and Mr. Ed Harris, respectively. In addition, Dr. Khusid discussed specific features of the operating conditions of the aircraft weapon and ground support equipment with Dr. Verma during the latter's visit to Beltran, Inc. Furthermore, having obtained from Dr. Verma the telephone numbers of Dr. Mark Milton and Mr. Brett Gardner, aircraft engineers, and Ms. Kitty Godburn, a chemist, Dr. Khusid telephoned them in order to discuss the operating conditions of the Navy equipment in more detail. Also, we consulted Prof. Markus Zahn, Massachusetts Institute of Technology (MIT), Cambridge, MA, an expert in the electro-hydrodynamics.

Based on the available cumulative data of Navy laboratories and the results of recent studies of the degradation of hydrocarbon fluids (briefly listed in Section 2.1.1), we evaluated that the following processes can influence the degradation of a PAO fluid under operating conditions of the electric equipment in Navy aircraft systems:

a) contamination with electro-corrosion and abrasion products,
b) aging caused by large temperature variations and mechanical stresses,
c) repetitive micro-discharge processes in proximity to high-voltage components,
d) flow and electric field induced electrification,
e) moisture adsorption.

As pointed out in Section 1, the NOAP test procedures and the corresponding commercially available pieces of equipment, which came into use primarily in the 80's for testing the properties of hydrolytically unstable Coolanol, appear to be inappropriate for the evaluation of the degradation of PAO fluid service properties under operating conditions. Accordingly, we concluded that the current status regarding the conversion of Navy aircraft systems to PAO fluids requires the development of new procedures for testing how the occurrence of severe service conditions could degrade the ability of such a fluid to withstand mechanical, temperature, and electrical stresses. The primary weakness of current test procedures employed by the Navy laboratories is that these tests are not based on reliable data concerning the degradation of the physical and chemical properties of a hydrolytically stable PAO fluid and, therefore, that these procedures are not sensitive enough to reveal a change in the PAO fluid properties under service conditions.

2.1.3. Setup for studying the degradation of PAO fluids in a recirculating flow

To perform experimental studies of the effects of mechanical, temperature, and electrical stresses on the degradation of a flowing PAO fluid, we constructed a recirculating setup which contains a fluid reservoir, a pump, a heater, an electric chamber, and a heat-exchanger (Figure 1). The flow and the electric field induced electrification of a fluid (the charge density entrained in a fluid flow) is monitored as the flow leaves the electric chamber. The parameters of these units were evaluated so as to expose a PAO fluid to electric fields, temperature variations, and mechanical stresses in the range similar to those of the Navy aircraft systems. This setup, filled with 5 gallons of a PAO fluid, has been operating continuously during the past several months with about 0.5-1.0 L of the fluid being sampled every two weeks.

To measure the flow and the electric field induced electrification of a PAO fluid, we used a portable absolute charge sensor (ACS) which has been developed at MIT [19, 20] for measuring the electrification of transformer oils and hydrocarbon fuels and which has been shown to be superior to other relevant techniques.

The portable ACS and its diagram are shown in Figure 2. This compact unit which incorporates the required sensitive electronics and signal conditioning procedures can be easily installed in field locations. The heart of the instrument is a metal container acting as a Faraday cage into which the fluid to be measured is drawn. This container is grounded through an

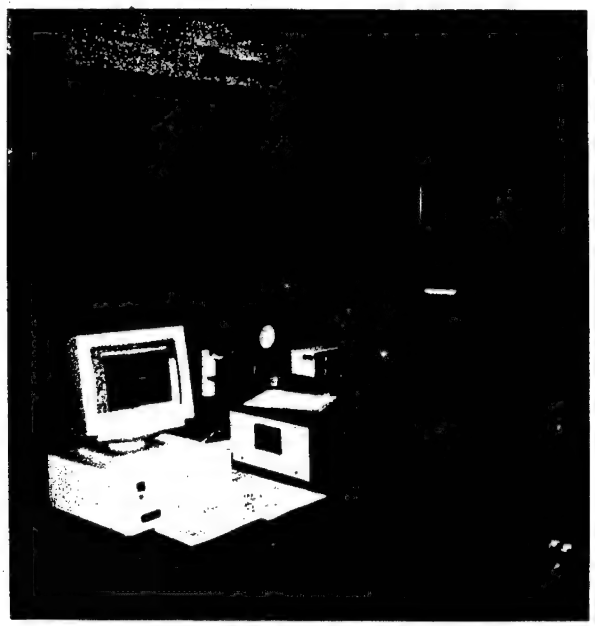

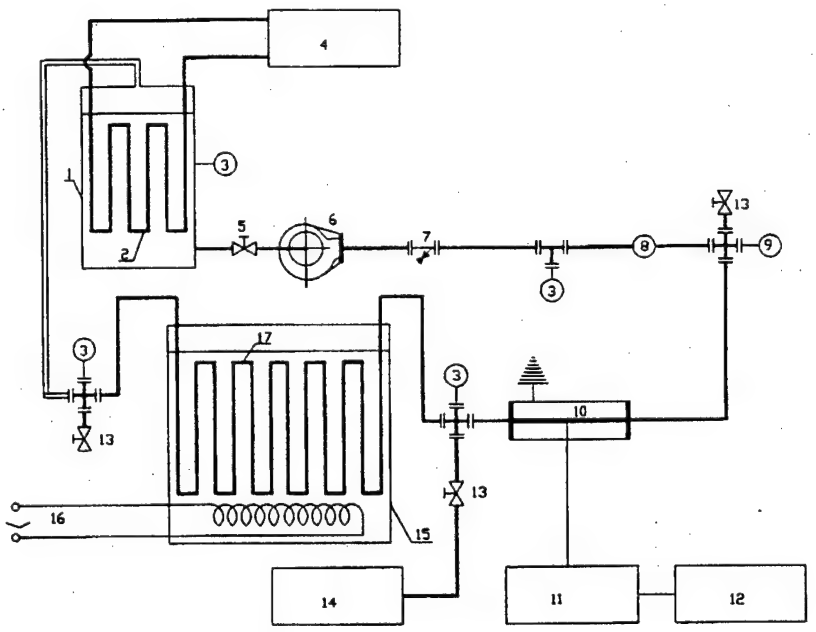

Figure 1. Lab-scale Setup for Studying PAO Fluid Degradation in a Recirculatory Flow, and its Flow Diagram.

1) 5-gallon tank filled with the PAO fluid; 2) Cooling fluid coil; 3) Thermometers; 4) Thermostatic unit filled with a transformer oil; 5) Valve for sampling the PAO fluid; 6) Gear-type pump; 7) Filter; 8) Flow meter; 9) Manometer; 10) Electric chamber; 11) Control unit; 12) 30 kV power supply; 13) Valve foron-*line* measuring the charge density in the PAO fluid flow; 14) Absolute charge sensor; 15) Tank filled with transformer oil; 16) Heater; 17) Coil for heating the PAO fluid.

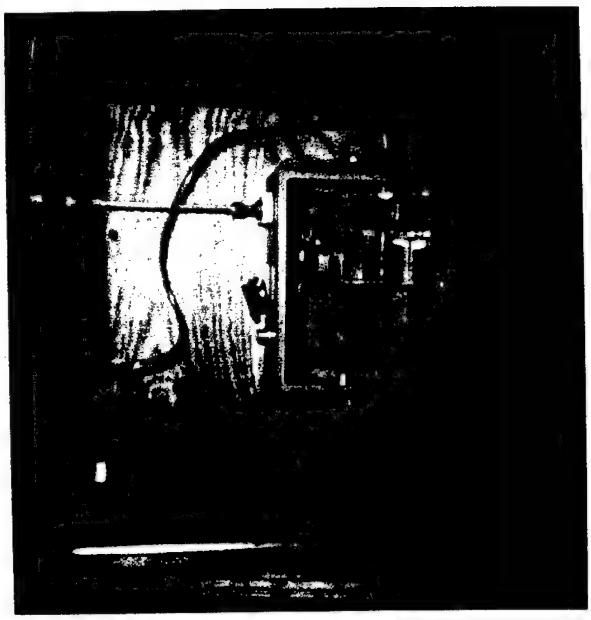

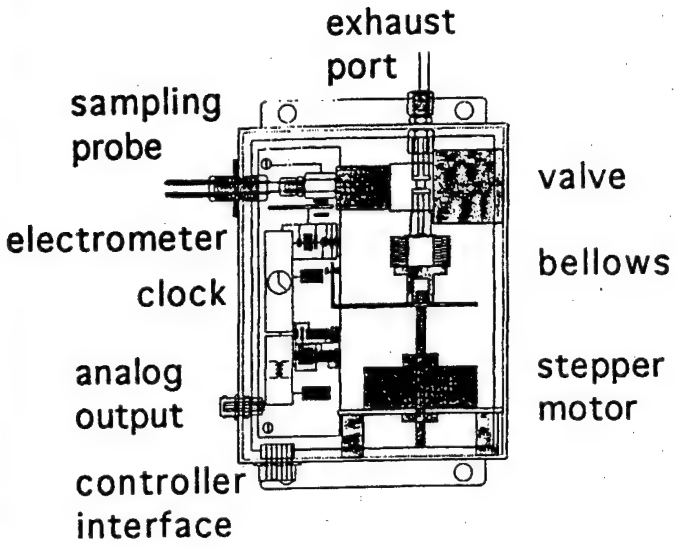

Figure 2. The Portable Absolute Charge Sensor (ACS), and its Diagram.

The inner conductor of the sampling probe connects to the inlet of the electrically actuated valve and the outer conductor connects to the grounded case.

electrometer. When a charged fluid is drawn into the container, a current flows to ground. The magnitude of this current is proportional to the amount of charge in the fluid and the rate at which the fluid is drawn in. A linear stepper motor is connected to a metal bellows to draw the fluid into the container and then to discharge this fluid when the measurement is completed. An optical sensor is used to determine the position of the bellows at the start of each measurement.

2.1.4. Setup for studying PAO fluid degradation under partial discharges

It is believed that partial discharges (PD) originate from various defects in the insulating liquid, such as fine particles and bubbles, within which an applied electric field could cause ionization that results in a displacement of charges and hence an electric current pulse [7-9]. PDs inevitably occur in the neighborhood of high-voltage elements, which are characteristic features of any high-power equipment, including the Navy aircraft systems as well.

Many different experimental arrangements have been used to assess the initial experiments. A sparking setup, shown in Figure 3, was constructed. This device consists of a vibrating electric chamber which is mounted on a slider-crank assembly and is equipped with needle electrodes located above an electrode plate; the needle-plate gap varied from 0.5 mm to 1mm. Mixing of the test fluid was achieved by vibrating the chamber with an amplitude of 0.25". This setup facilitates the simulation of types of PD in an electrically stressed dielectric liquid which originate from sharply edged high-voltage electrodes. The chamber filled with 180 ml of a PAO fluid can operate for several days under the application of voltages up to 20 kV.

2.1.5. Setup for the electrokinetic separation of PAO fluids

We exploited the electro-separation of PAO fluids for evaluating their degradation in Navy aircraft systems due to their contamination with fine carbonaceous particles caused by electro-corrosion, abrasion, aging, etc. Moreover, such a separator can be used for in site remediation of PAO fluids in aircraft equipment. A scheme of a novel electrokinetic separator (Figure 4) which we developed is based on a new concept [29, 30] for a continuous electro-separation technique which, by applying a non-uniform electric field to a flowing fluid, exploits the electric-field-induced aggregation and dielectrophoresis to remove contaminants from the flow. In this case, the non-uniform electric field is generated by two interdigitated electrode arrays placed on the opposite sides of a parallel-plate channel. The contaminated PAO fluid flows in a direction perpendicular to the electrode arrays (see Figure 4). Three outlet stream splitters are placed into the electric chamber in order to subdivide the liquid into layers at the exit of the channel so as to separate layers with different concentration of contaminant particles.

The geometrical parameters of the electrode arrays in the separator have been properly chosen in order to produce a high degree of electric field non-uniformity not only within the vicinity of the electrode tips but also within the main body of the channel. The dielectrophoretic force, which is exerted on a particle, points towards the center between the nearest electrodes or in the opposite direction depending on whether this particle has positive or negative polarizability, respectively. Correspondingly, this electric-field-induced particle redistribution across the flow will result in enriching the regions near the walls or at the center of the channel

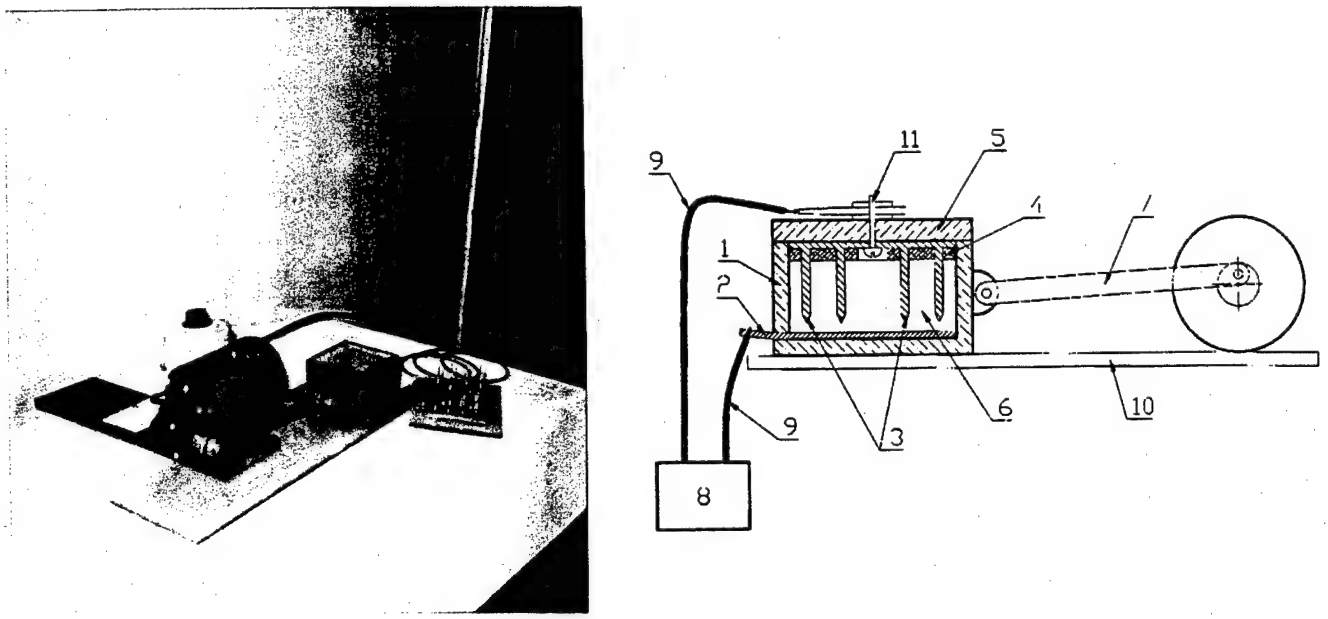

Figure 3. Lab-scale Setup for Studying PAO Fluid Degradation under Partial Discharges, and its Diagram.

1) 180 ml electric chamber; 2) Plate electrode; 3) 16 needle electrodes; 4) Insulator; 5) Chamber cover; 6) Test Fluid; 7) Slider-crank assembly; 8) High-voltage power supply; 9) High-voltage cables; 10) Base; 11) High-voltage connector.

The needle-plate gap is 1 mm. The amplitude of the chamber reciprocation motion is 0.25".

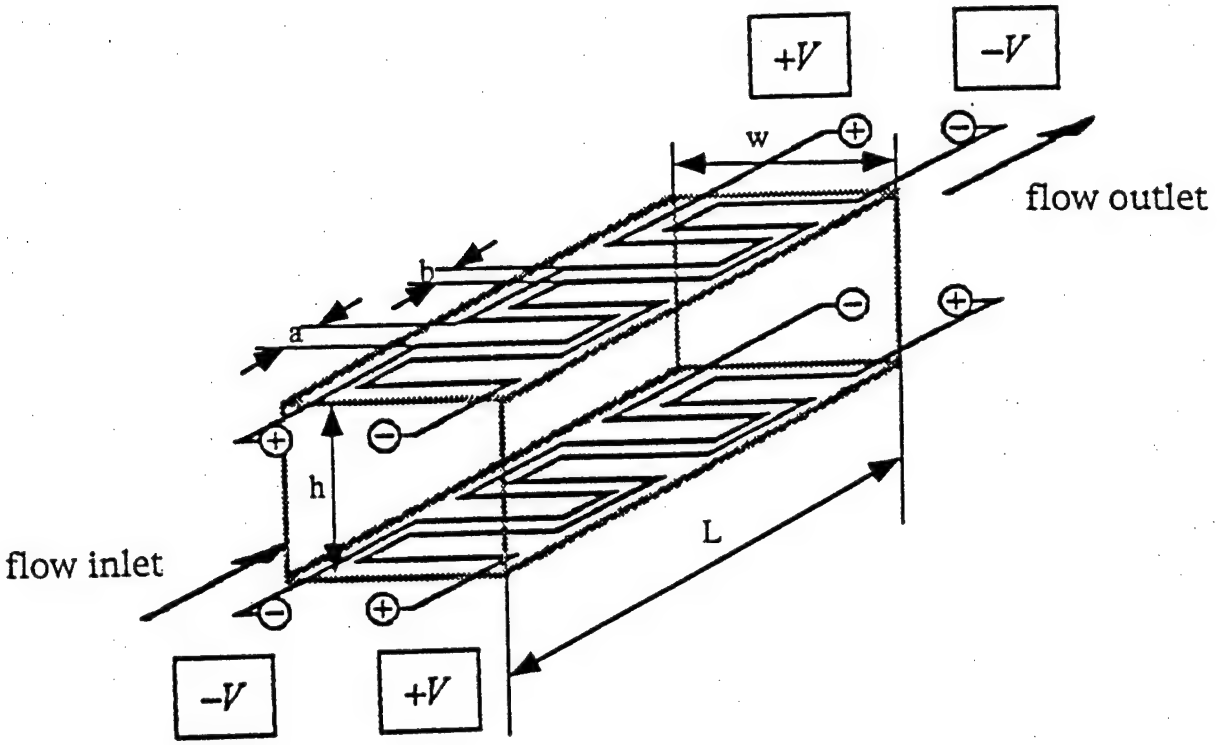

Figure 4. Electric Chamber with Interdigitated Electrode Arrays Placed on the Opposite Sides of a Parallel Plate Channel.

A contaminated PAO fluid will flow in a direction perpendicular to the electrode arrays.

with these contaminants. Moreover, their electric-field-induced aggregation can occur in these regions when the particle concentration exceeds a critical value; if so, the productivity of the particle separation will be significantly enhanced. To evaluate the geometrical parameters of the electrokinetic separator, we examined the Laplace equation which describes the spatial distribution of an electric field inside the chamber (Figure 4). We found that the geometrical parameters a/h and b/h of the electrode arrays (Figure 4) should range approximately from 0.5 to 0.7 with a set equal to b as a first approximation. The breadth-to-width ratio of the channel, w/h, should be larger than 4-5 in order to diminish the possibility of generating secondary flows perpendicular to the main flow. The length-to-width ratio, L/h, should be large enough, for example, 50-100, in order to easily vary the time of the particle motion through the channel by means of small variations in the applied pressure.

Figure 5 shows the interdigitated electrode arrays and the flow diagram of a lab-scale apparatus constructed by Beltran, Inc. The electric chamber is 3.7 mm × 15.7 mm × 200 mm. On leaving tank 1, the fluid sample is split into three portions which exit from the separate outlets at the exit of the separator and, thus, should contain different concentrations of contaminants. Once a fluid sample in tank 1 has passed through the device, the process is repeated with the effluents collected in tanks 4, 5, and 6.

2.2. Findings

2.2.1. Proposed procedures for evaluating PAO fluid degradation

As discussed in Section 1, the procedures which the Navy laboratories currently employ for testing PAO samples (water content, specific resistivity, dielectric strength, flash point, and particle contamination) appear to be inappropriate for evaluating the degradation of the PAO-fluid properties under service conditions typical of aircraft equipment. Therefore, we analyzed the currently available procedures that appear to be capable of measuring how strong electric fields, large temperature variations, and mechanical stresses degrade low-conducting non-polar liquids.

As a result of our studies, we found that, at present, it is not possible to conclusively identify procedures which are sensitive enough to evaluate the degradation of PAO fluids under specific operating conditions of Navy aircraft equipment, due to a shortage of currently available databases for this process. However, we identified the following four characteristics of PAO fluids and the methods appropriate to each test which appear to be sensitive enough to detect fluid degradation under mechanical, temperature, and electrical stresses in Navy aircraft systems.

Frequency dependence of a complex dielectric permittivity

The dielectric spectrum of a material is a representation of its complex dielectric permittivity, $\varepsilon^* = \varepsilon' - i\varepsilon''$, as a function of the frequency ω of an applied electric field [22]. The real component ε' gives the dielectric permittivity whereas the imaginary component ε'', equal to σ/ω with σ being the conductivity, determines the power dissipation (loss) in the material. For an ideal ohmic material, whose dielectric permittivity and conductivity are independent of

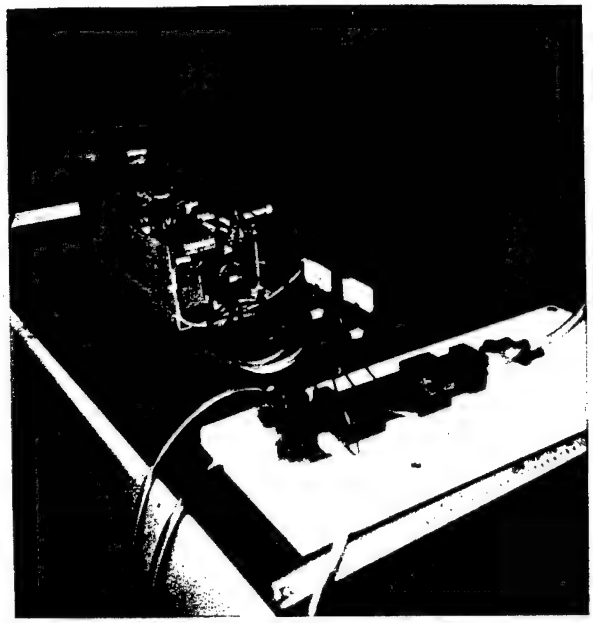

apparatus for electrokinetic separation

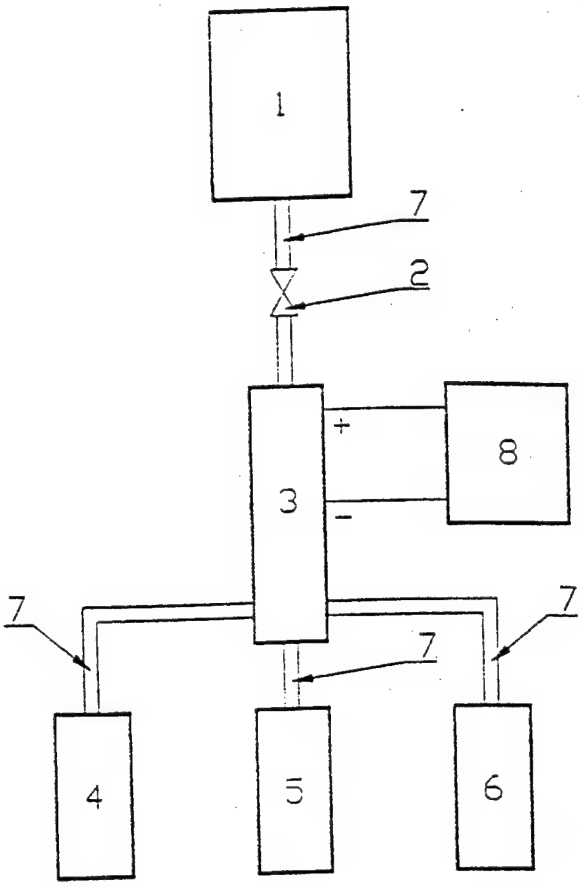

flow diagram

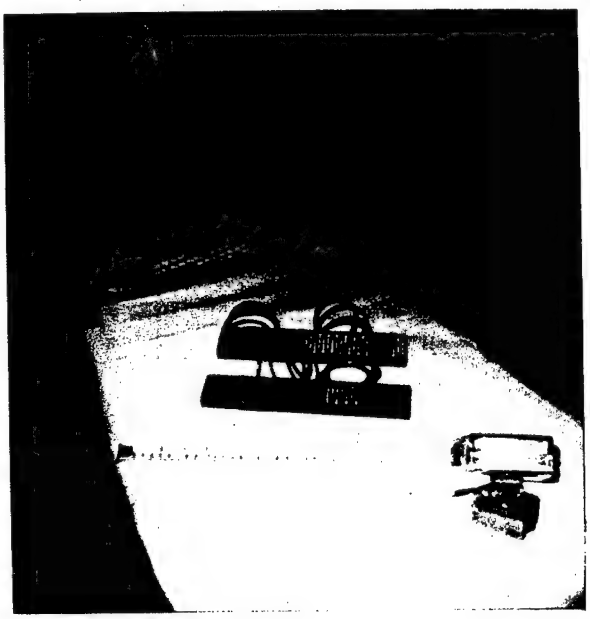

interdigitated electrode arrays

Figure 5. Lab-scale Apparatus for Electrokinetic Separation of Contaminated PAO Fluid Samples, its Interdigitated Electrode Arrays and Flow Diagram.

1) Tank filled with a fluid sample; 2) Valve; 3) Electric chamber equipped with interdigitated electrode arrays; 4), 5), and 6) Tanks for collecting effluents; 7) Pipes; 8) High-voltage power supply.

the frequency, a plot of $\log\varepsilon''$ vs. $\log\omega$ has a slope of -1. The dielectric spectrum reflects the various polarization processes in the material. Purified low-molecular weight liquids behave as ideal ohmic materials at frequencies below approximately 10^9 Hz. On the other hand, if such a fluid is contaminated, it will act as a dispersive material even below 10^9 Hz since its effective dielectric permittivity and conductivity will become frequency-dependent due to the polarization of the contaminants. The procedure for measuring the frequency dependence of the complex dielectric permittivity of a PAO fluid represents an extended version of the ASTM D 924-92 & D 150-95 test methods for the dissipation factor and the relative permittivity of insulating fluids.

The simultaneous measurement of the real and the imaginary components of the complex dielectric permittivity of a PAO fluid over a broad frequency range is more sensitive and thus more capable of providing information which can be correlated to the variation of the fluid properties during degradation than the measurement of the fluid specific resistivity by the ASTM D 1169-89 & D 257-93 test method which is currently in use in Navy laboratories (see Table 1).

Measurements of the dielectric spectrum of PAO fluid samples were performed at the Department of Chemical Engineering, Polytechnic University, Brooklyn, NY, using a Schlumberger Model 1260 impedance /gain phase analyzer.

Partial discharge inception voltage using needle-plane electrodes

International organizations such as CIGRE and IEC have attempted to develop techniques for evaluating dielectric liquids in terms of their insulating abilities [23-28]. Their attention focused on the concept of PD which has been used in the past to asses the quality of insulation materials. To quantify the use of PD, the lowest voltage at which such events could be detected, the so-called PD inception voltage (PDIV), was proposed by these organizations as such a measure. At present, many electrical laboratories exploit the measurement of the PDIV in their studies of discharge phenomena in insulating liquids.

Measuring the PDIV is more appropriate to the evaluation of the degradation of the PAO fluid dielectric strength in aircraft high-voltage systems than the ASTM D 1816-84A & D 877-87 test method currently in use in Navy laboratories (see Table 1) since the former (i) involves measurements of the lowest voltage at which micro-discharge events can be detected and (ii) is based on needle-plate electrodes which generate high-gradient electric fields typical of angular-featured elements of high-voltage equipment.

The procedure for the preliminary evaluation of PDIV PAO fluid samples makes use of a setup described in Sec. 2.1.4 in more detail. Measurements were performed by Beltran, Inc., staff.

Flow and electric field induced electrification

The ability of a flowing insulating liquid to transport and accumulate charges is one of the important fluid properties related to the failures of forced-cooled electrical equipment similar

to the one in the Navy aircraft systems. The procedure for measuring the electrification of a PAO fluid makes use of an ACS developed at MIT and is described in Section 2.1.3 in more detail. Measurements of the electrification of PAO fluid samples were performed by Beltran, Inc., staff.

Viscosity

Fluid viscosity governs the fluid flow rate which, in turn, determines the performance of the cooling equipment similar to that in aircraft systems.

The procedure for measuring the viscosity of a PAO fluid makes use of the Cannon-Fenske routine viscometer and is the same as that specified by the ASTM D 445-94 test method for the kinematic viscosity of liquid petroleum products. Measurements of the viscosity of PAO fluid samples were performed by Beltran, Inc., staff.

The procedures which have been proposed serve as useful indications of the changes in the quality of dielectric coolants resulting from their degradation in service, as they are very sensitive to small variations of ionic conductivity, water content, and of contamination with fine particles and bubbles. Moreover, they complement each other. Also, they do not require a large volume of specimen which is important since most of the aircraft systems contain rather small amounts of PAO fluids. In addition, these procedures are simpler, faster, and less expensive than measuring the water content by means of a Karl Fischer reagent (ASTM 1744-92 & D 1533-88 methods) or counting the particles by a laser-diode sensor, procedures that are currently being employed at the Navy laboratories for similar purposes (see Table 1).

We now consider the volume of test cells to be employed in the proposed procedures. In conformation with NOAP, the volume of a PAO fluid sample to be sent to the Navy testing laboratories is about 200 ml with about 100 ml for measuring its flash point. Thus only 100 ml of an incoming sample are available to test its other properties. We believe that an incoming sample should be divided into three or four specimens to allow one to calculate the average over several specimens as well as the probable error of their average both of which are required to determine whether the sample passes or fails the tests. In addition, one unused fluid sample should be stored in the laboratory for one to two weeks in case a customer decides to repeat the tests in another laboratory. Thus the volume of cells for testing properties of the PAO fluid should be about 16-20 ml if the measurements are to be performed in succession. Actually, the volume of the test cells for the proposed procedures could be made several times lower, thereby enabling one to make measurements in parallel.

2.2.2. Fluid decomposition caused by repetitive partial discharges (PD)

The PD experiments were carried out with the sparking setup shown in Figure 3. Fluid samples were exposed to a voltage ranging from 1 kV to 20 kV. We found that the electric breakdown in a PAO fluid results in the formation of fine (less than 1 μm) carbonaceous particles plus some flammable gas which more than likely is hydrogen. The rate of the fluid decomposition increases rapidly with the applied voltage.

2.2.3. Flow and electric field electrification

The experiments were carried out with the recirculating setup shown in Figure 1. Figures A1-A10 in the Appendix show some data concerning the time-variation of the charge density in the flowing PAO fluid in the recirculating setup. The data given in Figures A1-A9 correspond to the case when the central electrode in the electric chamber (Figure 1) was positive whereas the data in Figures A10 and A11 correspond to the case when this electrode was negative.

As can be seen from these data, flow electrification of the fluid generates a charge density of about $-100\mu C/m^3$ at room temperature in the absence of an applied electric field. The magnitude of this charge density in the flow decreases as the fluid temperature increases. The application of an electric field induces charge injection into the flowing fluid. At low electric fields, the injection of positive ions prevails. For example, the application of 2.67 kV/mm increases the charge density up to about $+20\mu C/m^3$ when the central electrode was positive and up to about $-7\mu C/m^3$ when this electrode was negative .For stronger fields, however, the injection of negative ions prevails, so then the charge density decreases monotonically to about - $+700\mu C/m^3$ at 11.7 kV/mm.

2.2.4. Dielectric spectrum, viscosity, transmittance in the ultra-violet (UV) and visible (VIS) light, infrared (IR) spectrum

We measured the frequency dependence of the real and the imaginary components of the complex dielectric permittivity of exposed PAO fluid samples that originated from the recirculating setup and of the non-exposed control, respectively (Figure A12). The data reported in Figure A12 demonstrate that some changes in the low-frequency magnitudes of the imaginary component ε'' with degradation have occurred.

Data on the viscosity of the exposed PAO fluid samples and of the non-exposed control, respectively, are depicted in Figure A13. These data demonstrate that some changes in the magnitudes of the viscosity with degradation under partial discharges have occurred.

We examined the transmittance of the exposed PAO fluid sample which originated from the both setups and of the non-exposed control, respectively. The measurements were performed by Beltran, Inc., staff.. These data reported in Figures A14 (a and b) demonstrate that the fluid degradation in a recirculatory setup has resulted in some decrease in the magnitude of UV and VIS light transmittance, specifically, in the wavelength range from $400\,cm^{-1}$ to $480\,cm^{-1}$. The fluid degradation in the sparking setup is significantly greater (Figures A15 and A16). In this case, the transmittance lowers in the wavelength range from 400 cm^{-1} to 960 cm^{-1} due to the presence of larger amounts of carbonaceous particles.

The IR spectra (Figure A17) of the exposed PAO fluid samples which originated from the recirculating setup and the sparking setup, as well as of the non-exposed control, respectively,

were measured at the Naval Air Warfare Center, Aircraft Division, Patuxent River, MD . It was found that the peaks in the 3000 to 2800 cm^{-1} frequency range and around 1500 cm^{-1} frequency which are related to C-C and C-H bonds keep their shape. It indicates that the exposure of the PAO fluid to electrical, thermal, and mechanical stresses under our test conditions has left the molecular structure of this fluid unchanged.

2.2.5. Dielectric strength

Experiments were performed with the sparking setup shown in Figure 3. To evaluate PDIV of a fluid sample, we measured the voltage which generates, on the average, 3 discharges per minute during over 15 minutes. To this end, the applied voltage was slowly increased from zero until this number of breakdowns occurred, and the corresponding value was recorded. The average value of 3 specimens was considered as the dielectric strength of a sample.

We tested the dielectric strength of the PAO fluid samples which originated from the recirculating setup (Figure 1) and the sparking setup (Figure 3) as well as of the non-exposed control. We found that the dielectric strengths of these samples were 2 kV, 1 kV, and 1.3 kV, respectively.

The dielectric strengths of the same samples were also measured using the standard procedure (see Table 1) at The Mid-Atlantic Regional Calibration & Materials Test Laboratories, NARF Norfolk, VA. However, it was found that values so obtained differed from one another by less than 10% (see Figure 6).

2.2.6. Electrokinetic separation

Experiments were conducted on PAO fluid samples which originated from the sparking setup (Figure 3) as well as on samples that originated from the recirculating setup (Figure 1). The former samples were considerably more contaminated with carbonaceous particles. The voltage applied to the electrokinetic separator was about 4kV. The flow rate of a sample through the electric chamber (Figure 4) varied from 1.2ml/min up to 25ml/min.

Figures A15 and A16 depict the experimental data for the fluid samples which originated from the sparking setup. The data on the transmittance of the exposed fluid sample and of its three portions which came out from the different outlets at the exit of the separator (the flow rate was 11ml/min) as well as the data from the non-exposed control are given in Figure A15. As can be seen, the transmittance of the all fluid portions coming out from the separator is rather close to that of the non-exposed control. This means that most of the carbonaceous particles were trapped at the electrodes, and, moreover, that the time it takes for the dielectric force to drive a particle across the channel towards the electrode is significantly smaller than the time of the flight of this particle through the separator at this flow rate. However, data reported in Figure A16 demonstrate that the transmittance of the fluid coming out from the separator gradually decreases as the fluid flow rate is increased.

BELTRAN COOLANT SAMPLES

	ORIGINAL	FROM THE LOOP	SPARKING CHAMBER
VOLUME RESISTIVITY			
TEMPERATURE	73	73	73
% HUMIDITY	45	45	45
CURRENT	0.005	0.001	0.003
VOLUME RESISTIVITY	3982	19308	6636
DIELECTRIC STRENGTH			
RUN 1	315	318	201
RUN 2	289	319	300
RUN 3	315	283	389
RUN 4	305	299	334
RUN 5	302	238	410
RUN 6	NA	240	INSUFF
RUN 7	NA	235	INSUFF
RUN 8	NA	234	INSUFF
RUN 9	NA	247	INSUFF
RUN 10	NA	237	INSUFF
AVERAGE	305	286	327
STD DEV	10.77961	33.01969	82.74478
STATION	0.035320	0.124134	0.253197
AUTOMATIC PARTICLE COUNTING			
5-10 MICRON	86942	37218	NA
10-25 MICRON	56888	26887	NA
25-50 MICRON	4023	3789	
50-100 MICRON	244	274	
OVER 100 MICRON	34	44	NA
TOTAL	148241		NA
CONCENTRATION		25.1	
OPEN CUP			INS

MIL-C-87252B SPECIFICATION LIMITS	
DIELECTRIC STRENGTH	35 KV
RESISTIVITY	1.0 x 10^10 ohm-cm
WATER	50 ppm
FLASH POINT	320 deg F.
PARTICULATE CONTAMINATION	
5- MICRON	<10000
MICRON	<1000
MICRON	<150
CRON	<20
ON	<5

GROUND SUPPORT EQUI	
DIELECTRIC	30KV
RESISTIVITY	10 x 10^10 ohm-cm
WATER	100 ppm
FLASH POINT	275 deg F.
CONTAMINA	
5-15 MICRON	<24000
15-25 MICRON	<5360
25-50 MICRON	<780
50-100 MICRON	<110
OVER 100 MICRON	<41

AIRCRAFT	
IC STRENGTH	30KV
TIVITY	4 x 10^10 ohm-cm
WATER	150 ppm
FLASH POINT	275 deg F.
PARTICULATE CONTAMINATION	
5-15 MICRON	<87000
15-25 MICRON	<21400
25-50 MICRON	<3130
50-100 MICRON	<110
OVER 100 MICRON	<11

draft

NOTES:

VOLUME - MEASUREMENTS IN MICRO AMPS - RESISTIVITY REPORTED x 10^10 ohm-cm

DIELECTRIC STRENGTH - IF STD/AVG OF 1ST FIVE RUNS EXCEEDS 1 THEN AN ADDITIONAL 5 RUNS WAS MADE ON A NEW FILLING OF CUP
THIS WAS DONE TO SEE IF FLUID TO DO THIS ON SAMPLE IDENTIFIED AS SPARKING CHAMBER.
MEASURED IN KILOVOLTS/MIL

INSUFF - INSUFFICIENT FLUID

AUTOMATIC PARTICLE COUNTING - THE ORIGINAL AND FROM THE LOOP SAMPLE BOTH PARTIALLY CLOGGED THE SENSOR AND HAD TO BE CLEANED BEFORE PROCEEDING
SUSPECT SAMPLE BOTTLES WERE NOT CLEANED OR IMPROPER SAMPLING TECHNIQUE.
DIFFERENTIAL COUNTS

OPTIONAL FORM 99 (7-90)
FAX TRANSMITTAL

To	From
JACOB KHODARKOVSKY	W ZDROJEWSKI
Dept./Agency	Phone #
BELTRAN INC	757-545-8819
Fax #	Fax #
718-253-9028	757-444-0683

NSN 7540-01-317-7368 5099-101 GENERAL SERVICES ADMINISTRATION

06/26/97

Figure 6. Test Results.

The carbonaceous particles trapped at the electrodes can then be easily removed by switching off the electric field and flushing a relatively small amount of fresh fluid through the chamber.

To examine whether the contamination of a PAO fluid with submicron particles under conditions typical of Navy aircraft systems could be detected using commercially available equipment, we sent four 15ml-specimens taken form the same PAO fluid samples to the Coulter Corporation, Particle Characterization Division, Miami, FL, and to the Wilks Enterprise, Inc., South Norwalk, CT. The Coulter Corporation manufactures a large variety of high-quality particle analyzers whereas the Wilks Enterprise specializes in the design and manufacturing of cost-effective infrared soot meters for field-based operation.

Two of these PAO fluid specimens (Table 2, A and C) were taken from fluid samples originated from the sparking and recirculating setups, respectively, whereas the other two (Table 2, B and D) were taken from the same fluid samples once they had passed through the separator (the flow rate was 1.2ml/min). It turned out, however, that Wilks's Infracal Soot Meter had failed to measure the fluid contamination due to the extreme low particle concentrations in all these specimens. At the Coulter Corporation, these specimens were analyzed by means of the Coulter N4 submicron particle size analyzer since a significantly larger fluid volume is required for other particle analyzers. As was reported, the measurements on the Coulter N4 analyzer were performed at several scattering angles. However, due to the low particle concentrations, the data obtained (see Table 2) were not good enough to yield a reliable conclusion about either the particle size or the particle concentration.

TABLE 2. COULTER N4 PLUS.

No	Specimen	Mean Diameter (μm)	Counts per Second
A	Exposed in the sparking setup	≈ 1.64	$\approx 3.8 \times 10^6$
B	A after treatment	≈ 0.41	$\approx 2.7 \times 10^5$
C	Exposed in the recirculating setup	≈ 1.63	$\approx 4.2 \times 10^4$
D	C after treatment	≈ 0.42	$\approx 2.8 \times 10^4$

As can be seen from Table 2, the average particle diameter for both exposed specimens was estimated at $1.6\,\mu$m whereas that for the treated specimens was estimated at $0.4\,\mu$m. The data on the total intensity of scattering (Table 2, counts per second) provide some insight into the relative change in the particle concentration due to the passage of a contaminated sample through the separator. Specifically, for the sample A, a tenfold decrease in the intensity was observed.

2.3. Main Conclusions

We found that

- Electrical breakdown in a PAO fluid results in the formation of submicron carbonaceous particles and some flammable gas which, more than likely, is hydrogen.
- An applied electric field generates significant streaming electrification in a PAO fluid. Specifically, the injection of positive ions prevails at low electric fields whereas the injection of negative ions prevails at strong electric fields.
- The Navy Oil Analysis Program (NOAP) procedures, which were developed in the 1980s for testing hydrolytically unstable silicate-ester-based fluids (Coolanol), fail to test the degradation of hydrolytically stable PAO fluids currently used by the Navy.
- The current Navy aircraft systems may have residual Coolanol present because sufficient flushing of these systems did not occur when Coolanol was replaced by PAO fluid. This requires that the current test procedures should remain in effect until new test methods are developed and implemented and the results validated.

The test procedures that we proposed (based on our studies of the electric-thermal-mechanical decomposition of a PAO fluid), specifically, all the following measurements of

1. the frequency dependence of a complex dielectric permittivity (dielectric spectrum),
2. the partial discharge inception voltage using needle-plane electrodes,
3. the viscosity in a thin capillary,
4. the transmittance in ultra-violet and visible light

appear to be sensitive enough to characterize the PAO fluid degradation under operating conditions typical of Navy aircraft systems: Moreover, these procedures are simpler, faster, and less expensive than those currently being employed at the Navy laboratories.

We developed a novel electro-separation technique which exploits the combined effects of electric-field-induced dielectrophoresis and aggregation of contaminants in a flowing fluid. Experimental data substantiate its ability to remove carbonaceous particles from a PAO fluid.

Our studies indicate that the development of an instrumentation and technique for the condition-based monitoring of in-use PAO fluids and their remediation should significantly improve the effectiveness and reduce the procurement and maintenance costs of aircraft systems.

3. Technical Objectives for Future Research and Development

Future R &D will prototype hardware and develop test procedures and specifications. Demonstrations and validation are planned.

In future R & D we plan to prototype the hardware for testing of the degradation of a dielectric coolant. The proposed system will be able to make the following measurements:

1. low-frequency dielectric spectrum,
2. PDIV using needle-plane electrodes,
3. viscosity,
4. concentration of fine (< 1μm) and large (>5μm) particles.

A conceptual design of these procedures is sketched in Figure 7. Preliminarily, it is planned that the method for measuring the flash point of a fluid currently in place at depots will remain unchanged. The methods and testing procedures to be developed shall make it possible to monitor the moisture content, dielectric strength, and particle contamination of a dielectric coolant. Moreover, they shall not require a large volume of specimens, which is important for field techniques, since most aircraft radar system personnel send only a small amount of a fluid to the depot. Our test method will allow reproducibility tests to be conducted be cause of the small volume involved. This factor alone will allow field personnel to have faith in the laboratory findings.

Approach and schedule of major events

- Develop a test method which is based on scientific facts and whose results are verifiable by damage control samples produced in simulated test rigs.
- Validate the test results using field trial. Run side by side tests to compare old and new test methods to gain support and confidence of field personnel.

We recognize the need to interface with a user from the beginning of future R & D, as in our Phase I effort. To this end, we plan to deliver the instruments to be fabricated to The Mid-Atlantic Regional Calibration & Materials Test Laboratories, NARF Norfolk, VA, The Materials Engineering Laboratory, Naval Air Depot, North Island, San Diego, CA, and the Naval Air Warfare Center, Aircraft Division, Patuxent River, MD, in order to begin side-by-side testing of new procedures. The new test method should require very little training, if any. By the interface explained here, we feel the transition to the new test method will be easy, effective, and economical. This shall help not only in the timely implementation of these procedures but in meeting acceptance from field personnel.

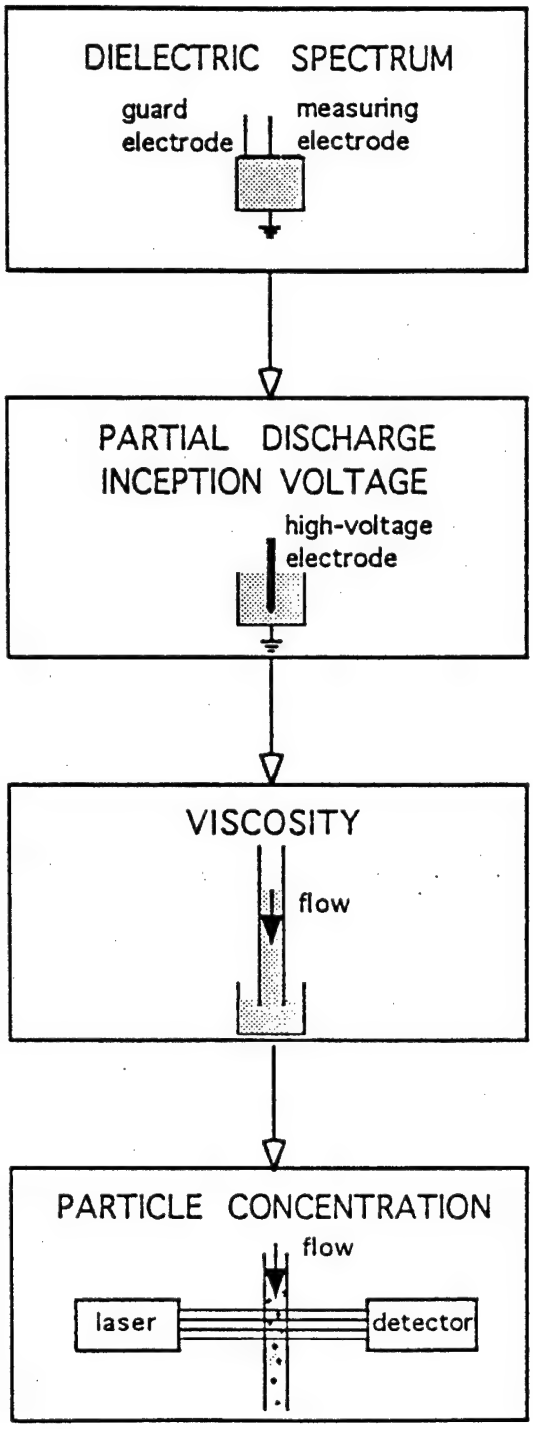

Figure 7. Conceptual Design of Test Procedures.
Volume of test cells is from 3 to 8 ml.

4. Commercialization Strategy

To identify commercial applications for the proposed technology, we have already performed a literature search over the Internet and the public library and then contacted several experts from relevant government agencies, universities, and companies. As a result, we have found that

- the major uses of PAO-based fluids thus far are forced-cooled electrical equipment in military and civilian aircraft and ground support systems. Furthermore, these fluids have found increasing favor as the best dielectric coolants in other industrial sectors, such as transformers and underwater cables. The market size is estimated at 20 million gallons, or approximately one billion dollars.
- there are well articulated expressions of dissatisfaction with the existing procedures for testing PAO-based fluids that lead to unreasonably shortened fluid lifetime.
- "wish list" performance standards for forced-cooled electrical equipment include cost-effective technology for the removal of the products of electro-corrosion, abrasion, and aging from a dielectric coolant.

The prototype of the proposed future R & D work will be equipment and methods for testing of PAO fluid degradation under service conditions of military and civilian aircraft and ground support forced-cooled electrical systems. There are no competing products to serve this market. Beltran considers that the hardware & procedure for testing and validation techniques will be applicable for the DOD and for private sector companies.

Beltran will demonstrate the end-use of the developed technology. We understand that no matter how unique our idea may be, and that even if the quality research we will accomplish should push the boundaries of knowledge, the main goal of our project will be to successfully bring the proposed technology to a ready-to-use condition and commercialize it. The purpose of the future R & D work is to develop a prototype from the Phase I R&D.

Beltran, Inc.'s commercialization strategy includes the collaboration of another company, Beltran Associates Inc., which has over 50 years designing, constructing, marketing and selling industrial electronic equipment to widely varied industrial sectors for a range of applications. Beltran Associates has designed, built and sold over 1000 systems worldwide. In addition to the North American market, Beltran is actively operating in Europe, Asia, Africa and Latin America. Beltran Associates sells worldwide directly through Beltran's sales engineers, as well as through a system of sales agents and distributors, all of whom would approach potentially interested industries with information on the availability and advantages of the PAO fluid degradation testing instrument. Beltran Associates also promotes its products through direct and magazine advertising, international trade shows, and technical conferences.

5. References

1. M.A. Stropki, *Polyalphaolefins: A new improved cost effective aircraft radar coolant*, Aeronautical Research Labs, Melbourne, Report No. ARL-MAT-R-124, (1991)
2. L. J. Gschwender et al., "Polyalphaolefins as candidate replacements for silicate ester dielectric coolants in military applications," *Lubrication Engineering*, 41, No. 4, 221 (1985)
3. *Coolant Fluid, Hydrolytically Stable, Dielectric*, MIL-C-87252B, Military Specification, 1996-05
4. *EMERY Polyalphaolefin Synthetic Lubricant Fluids*, EMERY Uncommon Chemicals, Cincinnati.
5. N. Felici, "High-field conduction in dielectric liquids revised," *IEEE Transaction on Electrical Insulation*, EI-20, No. 2, 233 (1985)
6. A.H. Sharbaugh et al., "Progress in the field of electrical breakdown in dielectric liquids," *IEEE Trans*. EI-13, 249 (1978)
7. E.O. Forster, "Progress in the field of electrical breakdown in dielectric fluids," *IEEE Transaction on Electrical Insulation*, EI-20, No. 2, 905 (1985)
8. E.O. Foster, "Progress in the understanding of electrical breakdown in condensed matter,". *J Phys. D: Appl. Phys*., 23, 1506 (1990)
9. J.K. Nelson, "Dielectric fluids in motion", *IEEE Electrical Insulation Magazine*, 10, No. 3, 16 (1994)
10. G. Theodossiou, J.K. Nelson, and G.M. Odell, "A computer simulation of transient electrodynamic motion in stressed dielectric liquids," *J. Phys. D: Appl. Phys*. 19, 1643 (1986)
11. G. Theodossiou, J.K. Nelson, M.J. Lee, and G.M. Odell, "The influence of electro-hydrodynamic motion on the breakdown of dielectric liquids," *J. Phys. D: Appl. Phys*. 21, 45 (1988)
12. J. Cuthbert, "Choose the right heat-transfer fluid," *Chemical Engineering Process*, July, 29 (1994)
13. R. Bozzo, G. Goletti, P. Molfino, and G. Molinari, "Electrode systems for dielectric strength tests controlling the electro-dielectrophoretic effect," *IEEE Transaction on Electrical Insulation*, EI-20, No. 2, 343 (1985)
14. A.P. Washabaugh and M. Zahn, "Charge density enhancement due to recirculatory flow," *IEEE Transaction on Dielectrics and Electrical Insulation*, 1, No. 1, 38 (1994)
15. R. Tamura, Y. Miura, T Watanabe, T. Ishii, M. Yamada, and T. Nitta, "Static electrification by forced oil flow in large power transformers," *IEEE Trans. Power Apparatus and Systems*, 99, No. 1, 335 (1980)
16. S.M. Gasworth, J.R. Melcher, and M. Zahn, "Flow-induced charge accumulation in thin insulating tubes," *IEEE Transaction on Electrical Insulation*, 23, No. 1, 103 (1988)
17. T.V. Oommen, "Static electrification properties of transformer oil," *IEEE Transaction on Electrical Insulation*, 23, 123 (1988)
18. J.K. Nelson and M.J. Lee, "Tandem-chamber charge density monitor," *Trans. IEEE*, EI-25, 399 (1990)

19. A.J. Morin II, M. Zahn, J.R. Melcher, and D.M. Otten, "An absolute charge sensor for fluid electrification measurement," *IEEE Transaction on Electrical Insulation*, 26, No. 2, 181 (1991)
20. J.R. Melcher, A.J. Morin II, and M. Zahn, *Method and apparatus for measurement of charge entrained in fluids*, U.S. Patent No. : 4,873,489 (1989)
21. H. Miyao, M. Higaki, and Y. Kamata, "Influence of AC and DC fields on streaming electrification of transformer oil," *IEEE Transaction on Electrical Insulation*, 23, 129 (1988)
22. A.K. Jonscher, *Dielectric Relaxation in Solids*. (Chelsea Dielectrics Press, London, 1983)
23. E.O. Forster, "Partial discharge and streamers in liquid dielectrics. The significance of the inception voltage," *IEEE Transaction on Electrical Insulation*, 28 No. 6, 941 (1993)
24. W.G. Chadband and T.M. Sufian, "Experimental support for a model of positive streamer propagation in liquid insulation," *IEEE Transaction on Electrical Insulation*, EI-20, No. 2, 239 (1985)
25. J.C. Devins et al., "Breakdown and prebreakdown phenomena in liquids," *J. Appl. Phys.*, 52, 4531 (1981)
26. R.E. Hebner et al., "Observations of prebreakdown and breakdown phenomena in liquid hydrocarbons," *J. Electrostatics*, 12, 265 (1982)
27. F. Oswath, E. Carminati, and A. Gandelli, "A contribution to the traceability of partial discharge measurements," *IEEE Transaction on Electrical Insulation*, 27, 130 (1992)
28. H. Yamashita, "Partial discharge measurements in dielectric liquids under impulse voltage," *IEEE Transaction on Electrical Insulation*, 28, No. 6, 947 (1993)
29. B. Khusid and A. Acrivos, "Effects of conductivity in electric-field-induced aggregation in electrorheological fluids," *Phys. Rev. E* , 52, 1669 (1995)
30. B. Khusid and A. Acrivos, "Effects of the interparticle electric interactions on dielectrophoresis in suspensions," *Phys. Rev. E* , 54, 5428 (1996)
31. C. H. Byers and A. Amarnath, "Understanding the potential of electro-separation," *Chemical Engineering Process*, February, 63 (1995)
32. M. Washizu, S. Suzuki, O. Kurosawa, T. Nishizaka, and T. Shinohara, "Molecular dielectrophoresis of biopolymers," *IEEE Trans. Ind. Appl.*, 30, 835 (1994))
33. H R.F. Becker, X.-B. Wang, Y. Huang,, R. Pethig, J. Vykoukal, and P.R.C. Gascoyne, "The removal of human leukemia cells from blood using interdigitated microelectrodes," *J. Phys. D: Appl. Phys.*, 27, 2659 (1994)
34. G.H. Marx and R. Pethig, "Dielectrophoretic separation of cells: continuous separation," *Biotechnology and Bioengineering*, 45, 337 (1995)

Appendix

Experimental Data

Appendix. Experimental Data

Figure Captions

Figure A1. Measurement of charge density in a recirculating PAO fluid as the flow leaves the electric chamber in the absence of an electric field. The flow rate $Q = 1.32\,L/\min$, the fluid temperature in the reservoir and in the electric chamber $T = 65F$.

Figure A2. Measurement of charge density in a recirculating PAO fluid as the flow leaves the electric chamber in the absence of an electric field. The flow rate $Q = 1.32\,L/\min$, the fluid temperature in the electric chamber $T = 125F$, and the fluid temperature in the reservoir is 65F.

Figure A3. Measurement of charge density in a recirculating PAO fluid as the flow leaves the electric chamber. The strength of the electric field in the chamber $E = 1.33\,kV/mm$ for the positive central electrode in the electric chamber, the flow rate $Q = 1.32\,L/\min$, the fluid temperature in the electric chamber $T = 83F$, and the fluid temperature in the reservoir is 65F.

Figure A4. Measurement of charge density in a recirculating PAO fluid as the flow leaves the electric chamber. The strength of the electric field in the chamber $E = 2.67\,kV/mm$ for the positive central electrode in the electric chamber, the flow rate $Q = 1.32\,L/\min$, the fluid temperature in the electric chamber $T = 83F$, and the fluid temperature in the reservoir is 65F.

Figure A5. Measurement of charge density in a recirculating PAO fluid as the flow leaves the electric chamber. The strength of the electric field in the chamber $E = 4.0\,kV/mm$ for the positive central electrode in the electric chamber, the flow rate $Q = 1.32\,L/\min$, the fluid temperature in the electric chamber $T = 83F$, and the fluid temperature in the reservoir is 65F.

Figure A6. Measurement of charge density in a recirculating PAO fluid as the flow leaves the electric chamber. The strength of the electric field in the chamber $E = 6.0\,kV/mm$ for the positive central electrode in the electric chamber, the flow rate $Q = 1.32\,L/\min$, the fluid temperature in the electric chamber $T = 83F$, and the fluid temperature in the reservoir is 65F.

Figure A7. Measurement of charge density in a recirculating PAO fluid as the flow leaves the electric chamber. The strength of the electric field in the chamber $E = 8.33\,kV/mm$ for the positive central electrode in the electric chamber, the flow rate $Q = 1.32\,L/\min$, the fluid temperature in the electric chamber $T = 83F$, and the fluid temperature in the reservoir is 65F.

Figure A8. Measurement of charge density in a recirculating PAO fluid as the flow leaves the electric chamber. The strength of the electric field in the chamber $E = 10.0\,kV/mm$ for the positive central electrode in the electric chamber, the flow rate $Q = 1.32\,L/\min$, the fluid temperature in the electric chamber $T = 83F$, and the fluid temperature in the reservoir is 65F.

Figure A9. Measurement of charge density in a recirculating PAO fluid as the flow leaves the electric chamber. The strength of the electric field in the chamber $E = 11.7\,kV/mm$ for the positive central electrode in the electric chamber, the flow rate $Q = 1.32\,L/\min$, the fluid temperature in the electric chamber $T = 83F$, and the fluid temperature in the reservoir is 65F.

Figure A10. Measurement of charge density in a recirculating PAO fluid as the flow leaves the electric chamber. The strength of the electric field in the chamber $E = 2.67\,kV/mm$ for the negative central electrode in the electric chamber, the flow rate $Q = 1.32\,L/\min$, the fluid temperature in the electric chamber $T = 83F$, and the fluid temperature in the reservoir is 65F.

Figure A11. Measurement of charge density in a recirculating PAO fluid as the flow leaves the electric chamber. The strength of the electric field in the chamber $E = 4.0\,kV/mm$ for the negative central electrode in the electric chamber, the flow rate $Q = 1.32\,L/\min$, the fluid temperature in the electric chamber $T = 83F$, and the fluid temperature in the reservoir is 65F.

Figure A12. Frequency dependence of the real and the imaginary components of the complex dielectric permittivity of two exposed PAO fluid samples which originated from the recirculating setup and of the non-exposed control.

Figure A13. Viscosity of the exposed PAO fluid samples and of ($\circ$) the non-exposed control; $\times$, samples originated from the recirculating setup and $*$, samples originated from the sparking setup.

Figure A14. Transmittance of the exposed PAO fluid samples originated from the recirculating setup at different times of exposure and of the non-exposed control; (a) the wavelength range from $320\,cm^{-1}$ to $960\,cm^{-1}$ and (b) its enlarged portion from $320\,cm^{-1}$ to $520\,cm^{-1}$.

Figure A15. Transmittance of the exposed PAO fluid sample originated from the sparking setup and of its three fluid portions which came out from the different outlets at the exit of the separator (the flow rate 11ml/min, the applied voltage 3.8kV) as weil as of the non-exposed control.

Figure A16. Transmittance of the exposed PAO fluid sample originated from the sparking setup and of its portions coming out of the separator at different flow rates as well of the non-exposed control.

Figure A17. The IR spectra of the exposed PAO fluid samples originated from the recirculating setup and the sparking setup, as well as of the non-exposed control.

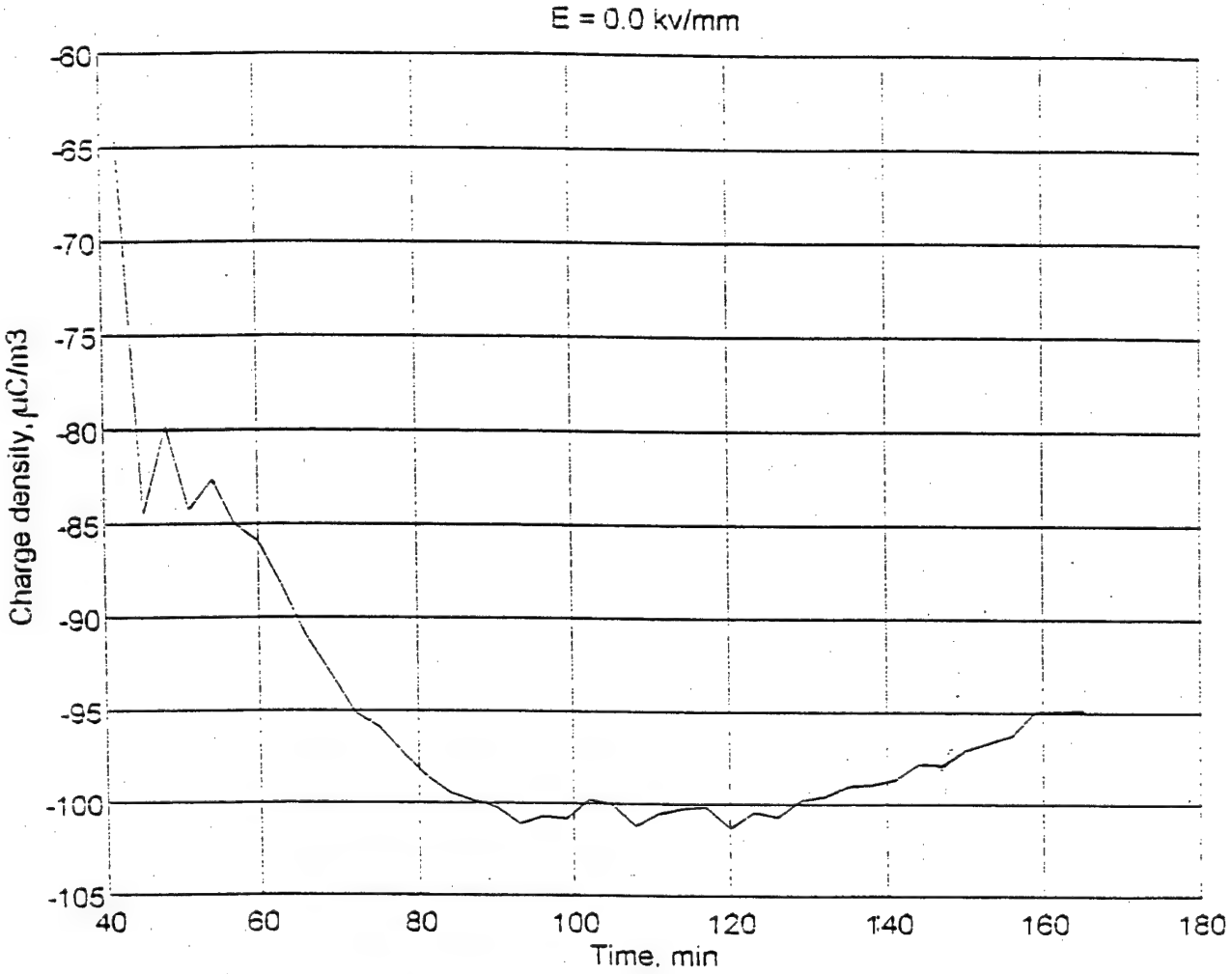

Figure A1. Measurement of charge density in a recirculating PAO fluid as the flow leaves the electric chamber in the absence of an electric field. The flow rate $Q = 1.32\,\mathrm{L/min}$, the fluid temperature in the reservoir and in the electric chamber $T = 65\mathrm{F}$.

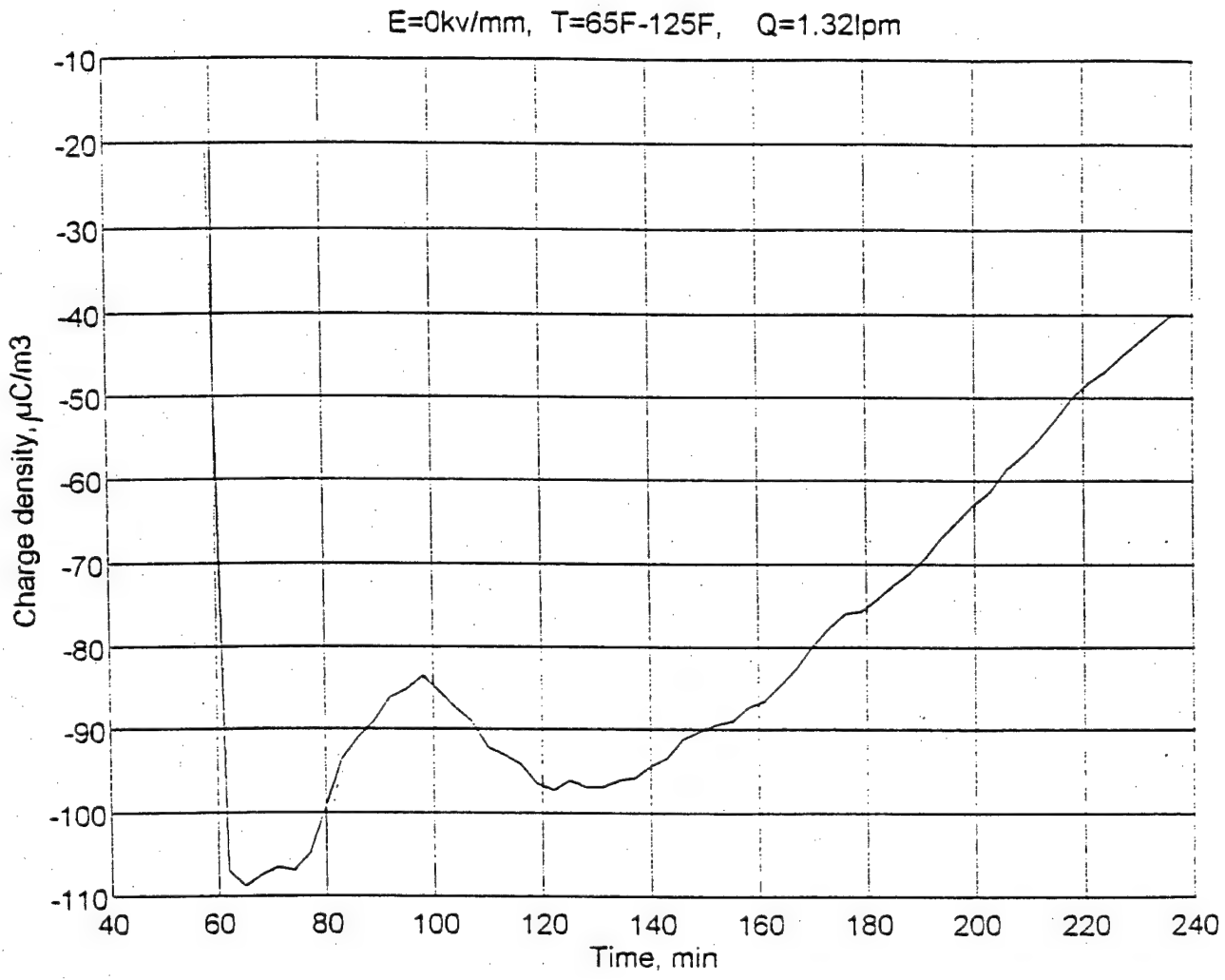

Figure A2. Measurement of charge density in a recirculating PAO fluid as the flow leaves the electric chamber in the absence of an electric field. The flow rate $Q = 1.32 L/\min$, the fluid temperature in the electric chamber $T = 125F$, and the fluid temperature in the reservoir is 65F.

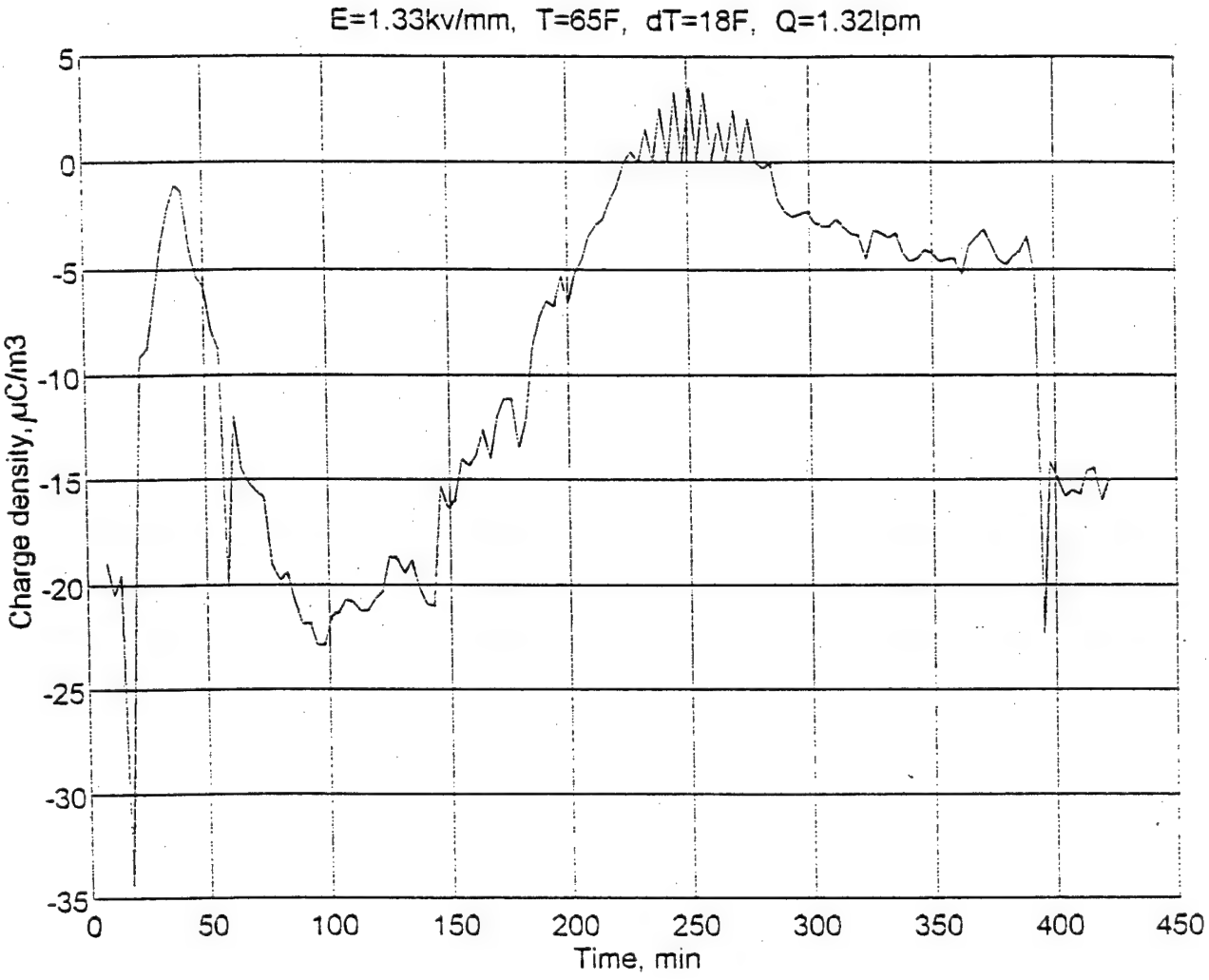

Figure A3. Measurement of charge density in a recirculating PAO fluid as the flow leaves the electric chamber. The strength of the electric field in the chamber $E = 1.33 kV/mm$ for the positive central electrode in the electric chamber, the flow rate $Q = 1.32 L/\min$, the fluid temperature in the electric chamber $T = 83F$, and the fluid temperature in the reservoir is 65F.

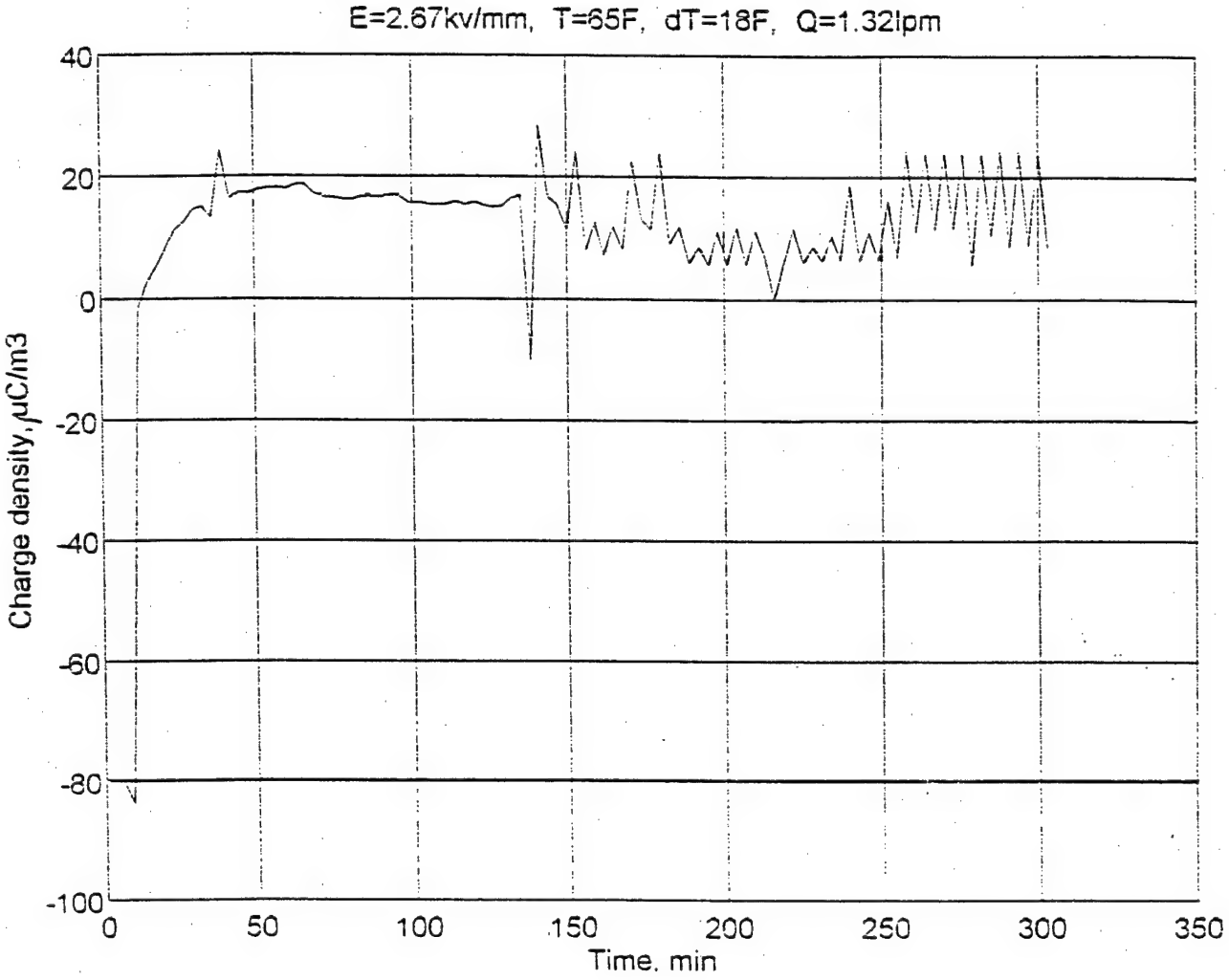

Figure A4. Measurement of charge density in a recirculating PAO fluid as the flow leaves the electric chamber. The strength of the electric field in the chamber $E = 2.67\,kV/mm$ for the positive central electrode in the electric chamber, the flow rate $Q = 1.32\,L/\min$, the fluid temperature in the electric chamber $T = 83F$, and the fluid temperature in the reservoir is 65F.

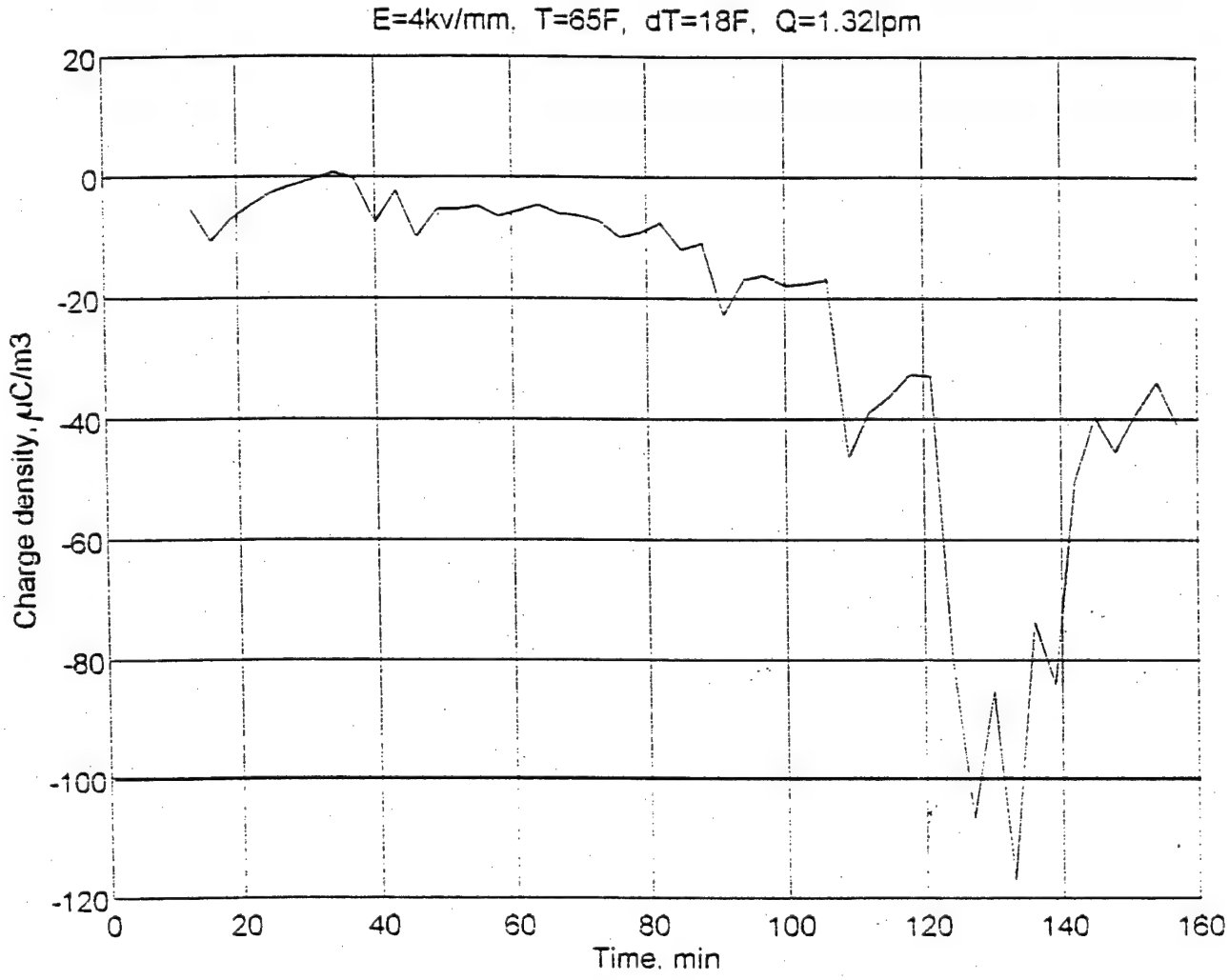

Figure A5. Measurement of charge density in a recirculating PAO fluid as the flow leaves the electric chamber. The strength of the electric field in the chamber $E = 4.0 kV/mm$ for the positive central electrode in the electric chamber, the flow rate $Q = 1.32 L/\min$, the fluid temperature in the electric chamber $T = 83F$, and the fluid temperature in the reservoir is 65F.

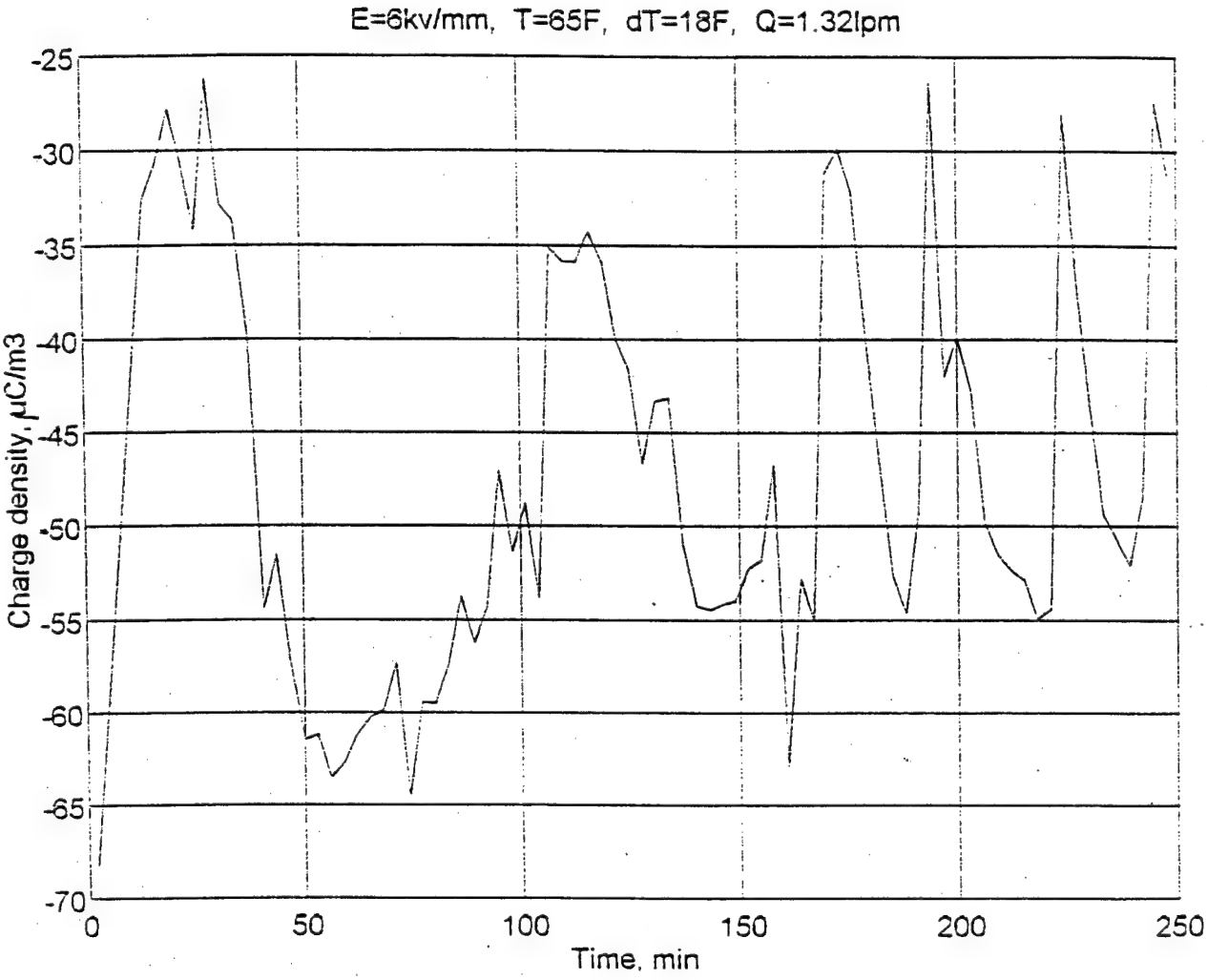

Figure A6. Measurement of charge density in a recirculating PAO fluid as the flow leaves the electric chamber. The strength of the electric field in the chamber $E = 6.0 kV/mm$ for the positive central electrode in the electric chamber, the flow rate $Q = 1.32 L/\min$, the fluid temperature in the electric chamber $T = 83F$, and the fluid temperature in the reservoir is 65F.

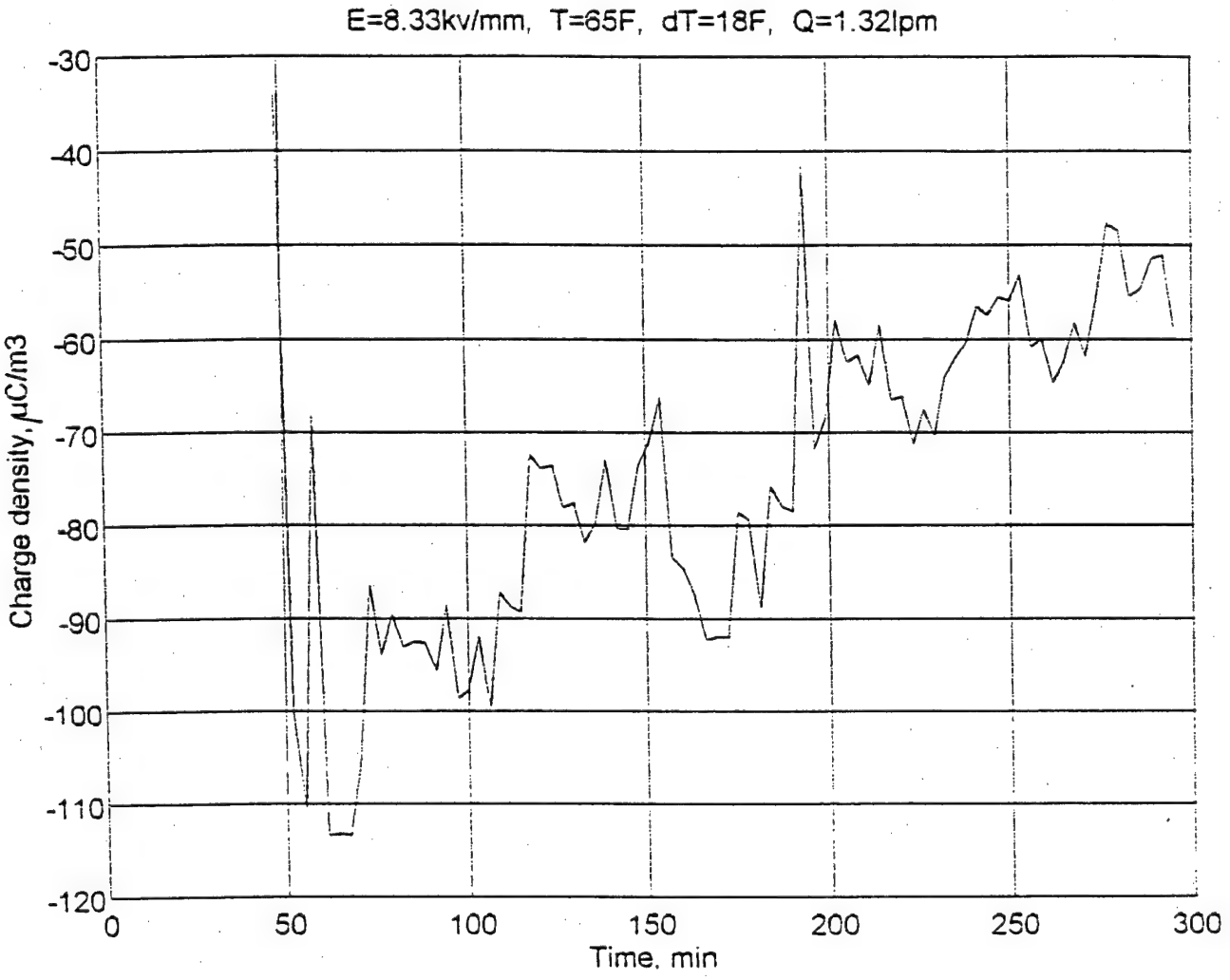

Figure A7. Measurement of charge density in a recirculating PAO fluid as the flow leaves the electric chamber. The strength of the electric field in the chamber $E = 8.33 kV/mm$ for the positive central electrode in the electric chamber, the flow rate $Q = 1.32 L/\min$, the fluid temperature in the electric chamber $T = 83F$, and the fluid temperature in the reservoir is 65F.

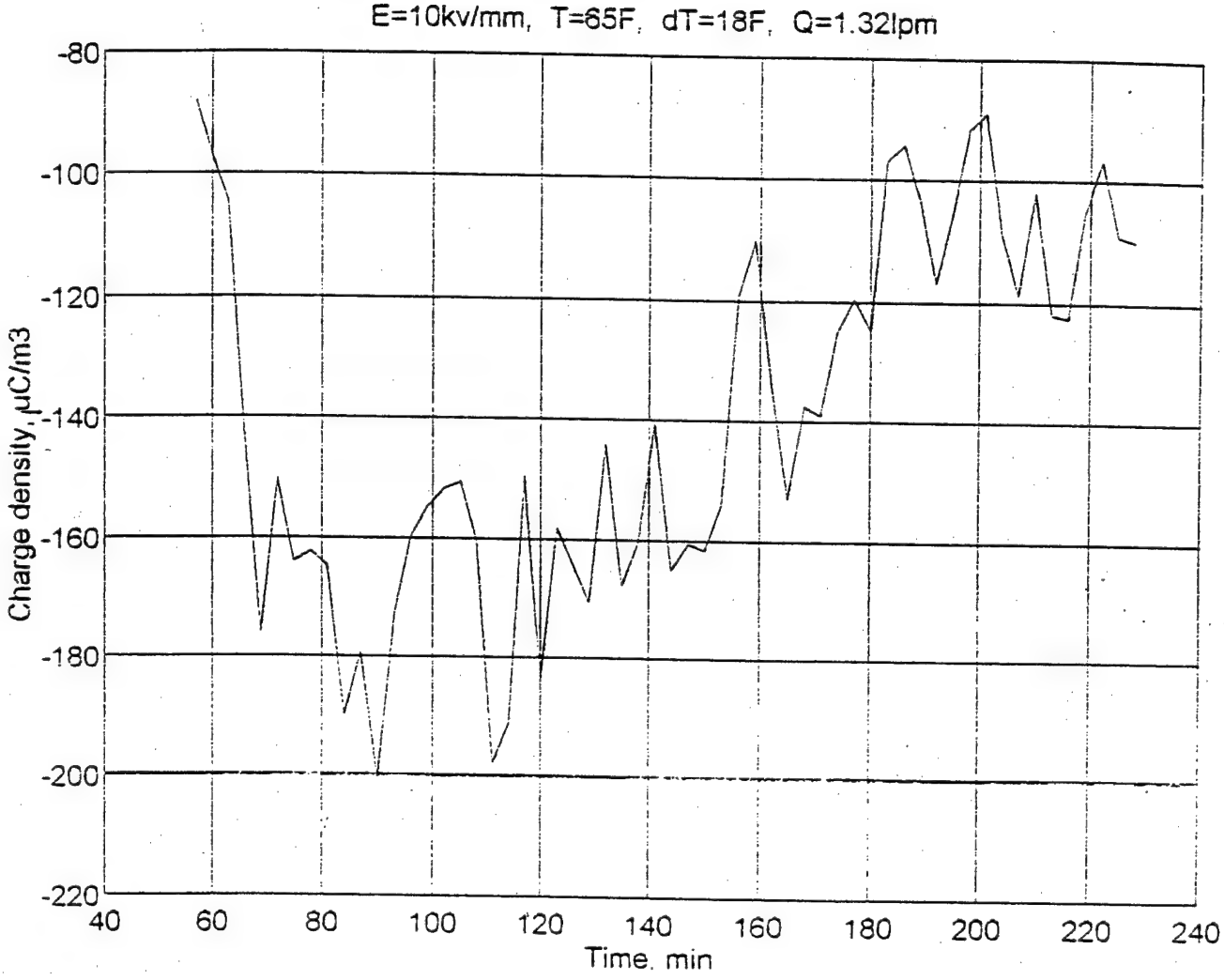

Figure A8. Measurement of charge density in a recirculating PAO fluid as the flow leaves the electric chamber. The strength of the electric field in the chamber $E = 10.0\,kV/mm$ for the positive central electrode in the electric chamber, the flow rate $Q = 1.32\,L/\min$, the fluid temperature in the electric chamber $T = 83F$, and the fluid temperature in the reservoir is 65F.

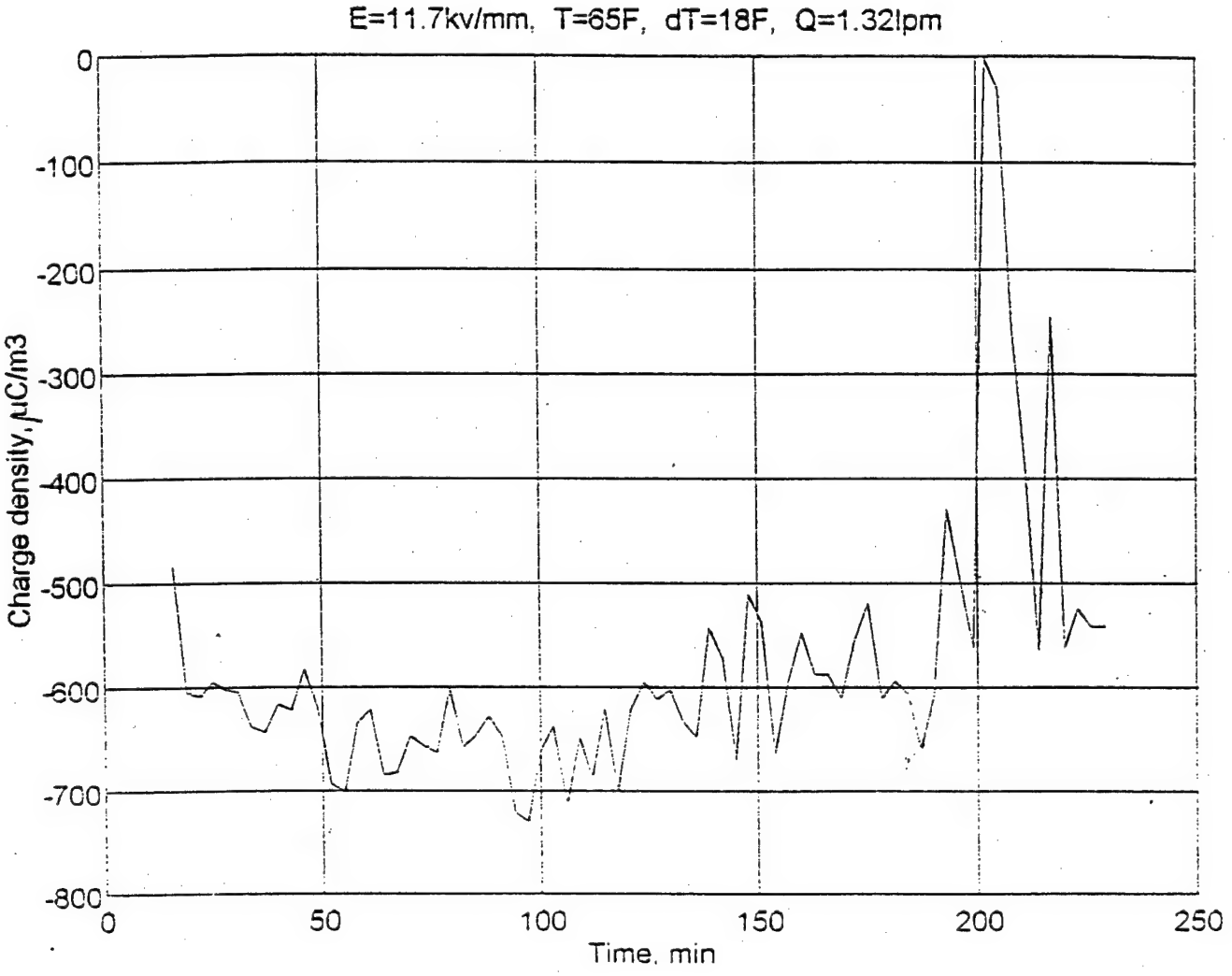

Figure A9. Measurement of charge density in a recirculating PAO fluid as the flow leaves the electric chamber. The strength of the electric field in the chamber $E = 11.7\,kV/mm$ for the positive central electrode in the electric chamber, the flow rate $Q = 1.32\,L/\min$, the fluid temperature in the electric chamber $T = 83F$, and the fluid temperature in the reservoir is 65F.

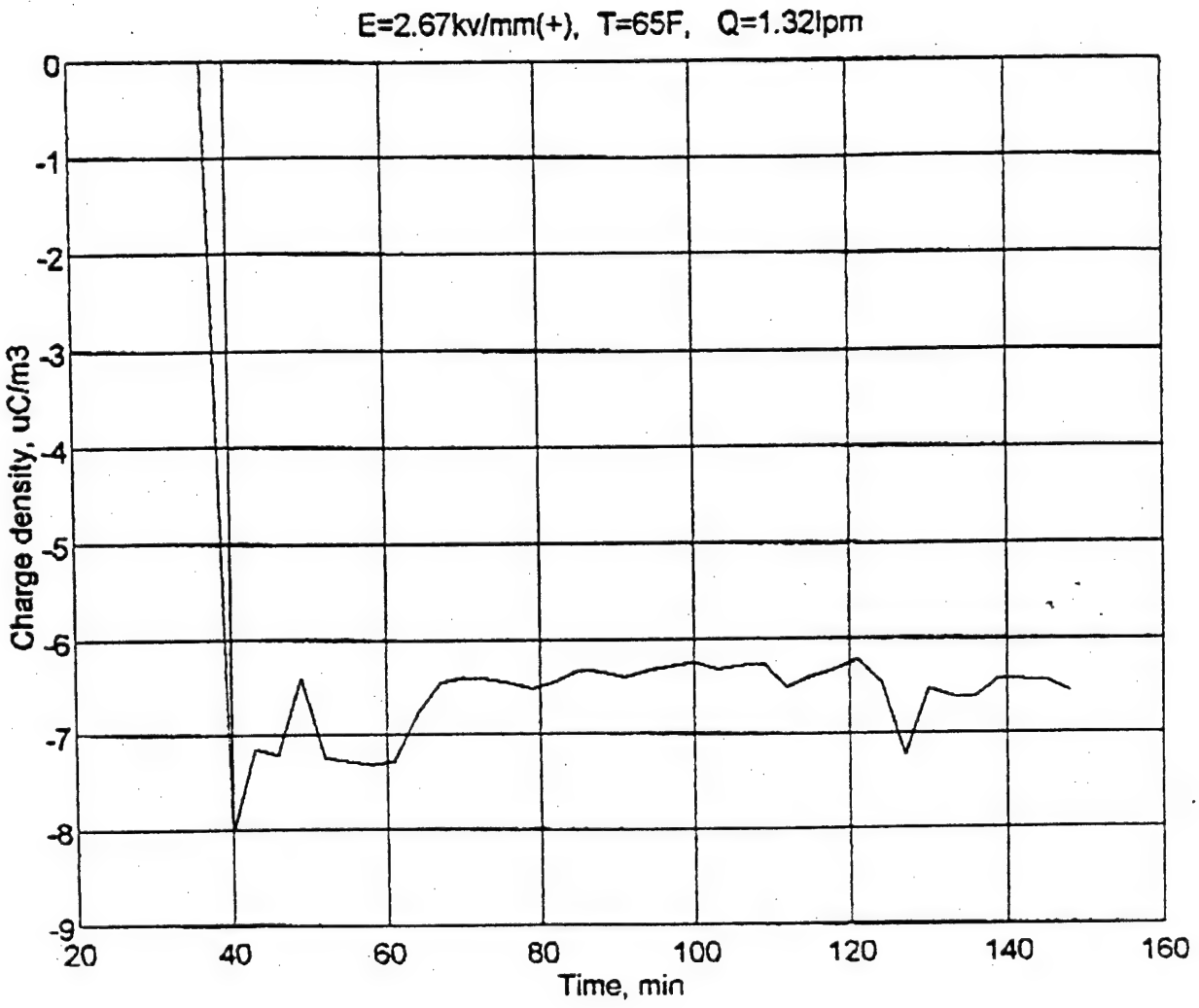

Figure A10. Measurement of charge density in a recirculating PAO fluid as the flow leaves the electric chamber. The strength of the electric field in the chamber $E = 2.67\,kV/mm$ for the negative central electrode in the electric chamber, the flow rate $Q = 1.32\,L/\min$, the fluid temperature in the electric chamber $T = 83F$, and the fluid temperature in the reservoir is 65F.

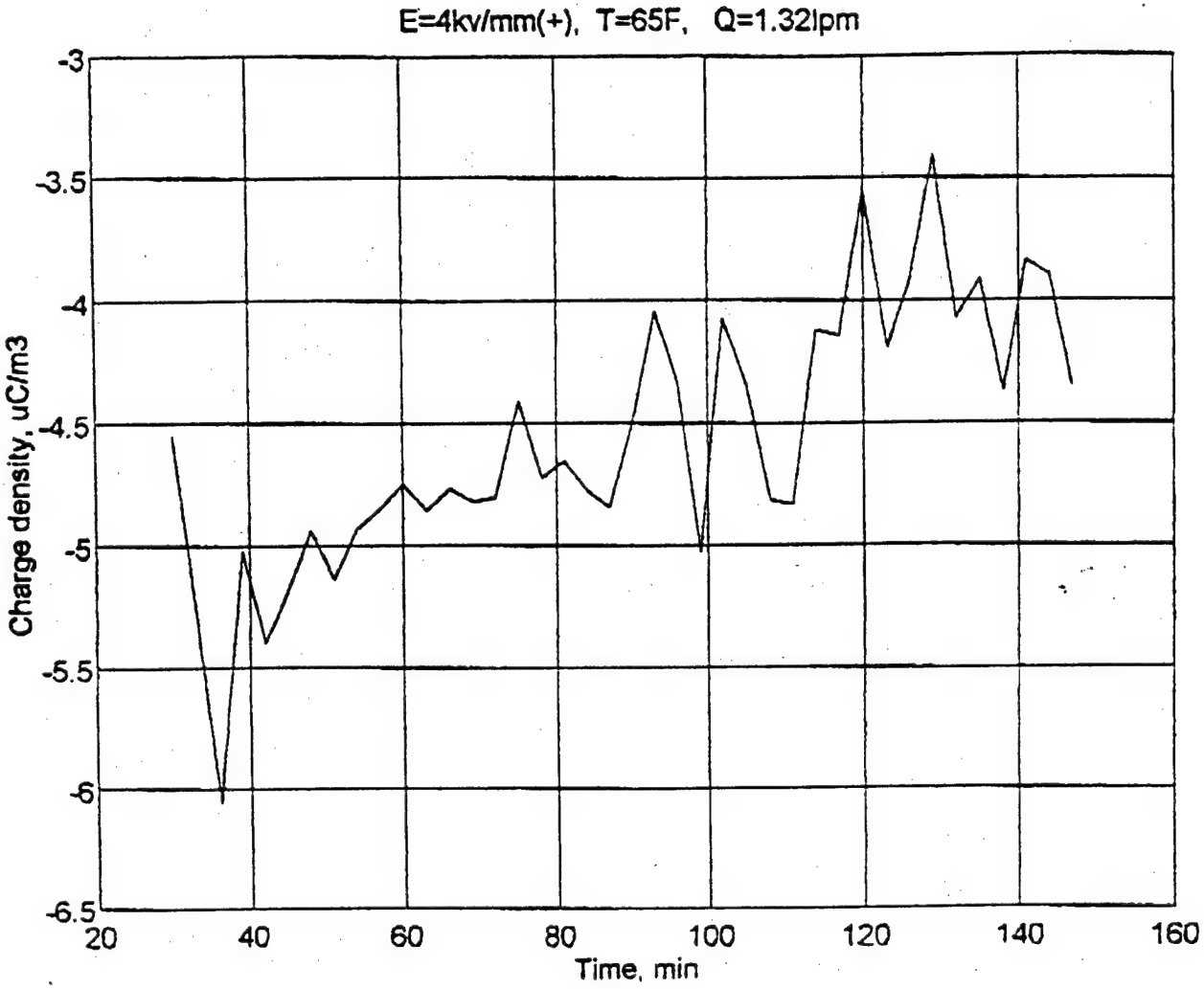

Figure A11. Measurement of charge density in a recirculating PAO fluid as the flow leaves the electric chamber. The strength of the electric field in the chamber $E = 4.0 kV/mm$ for the negative central electrode in the electric chamber, the flow rate $Q = 1.32 L/\min$, the fluid temperature in the electric chamber $T = 83F$, and the fluid temperature in the reservoir is 65F.

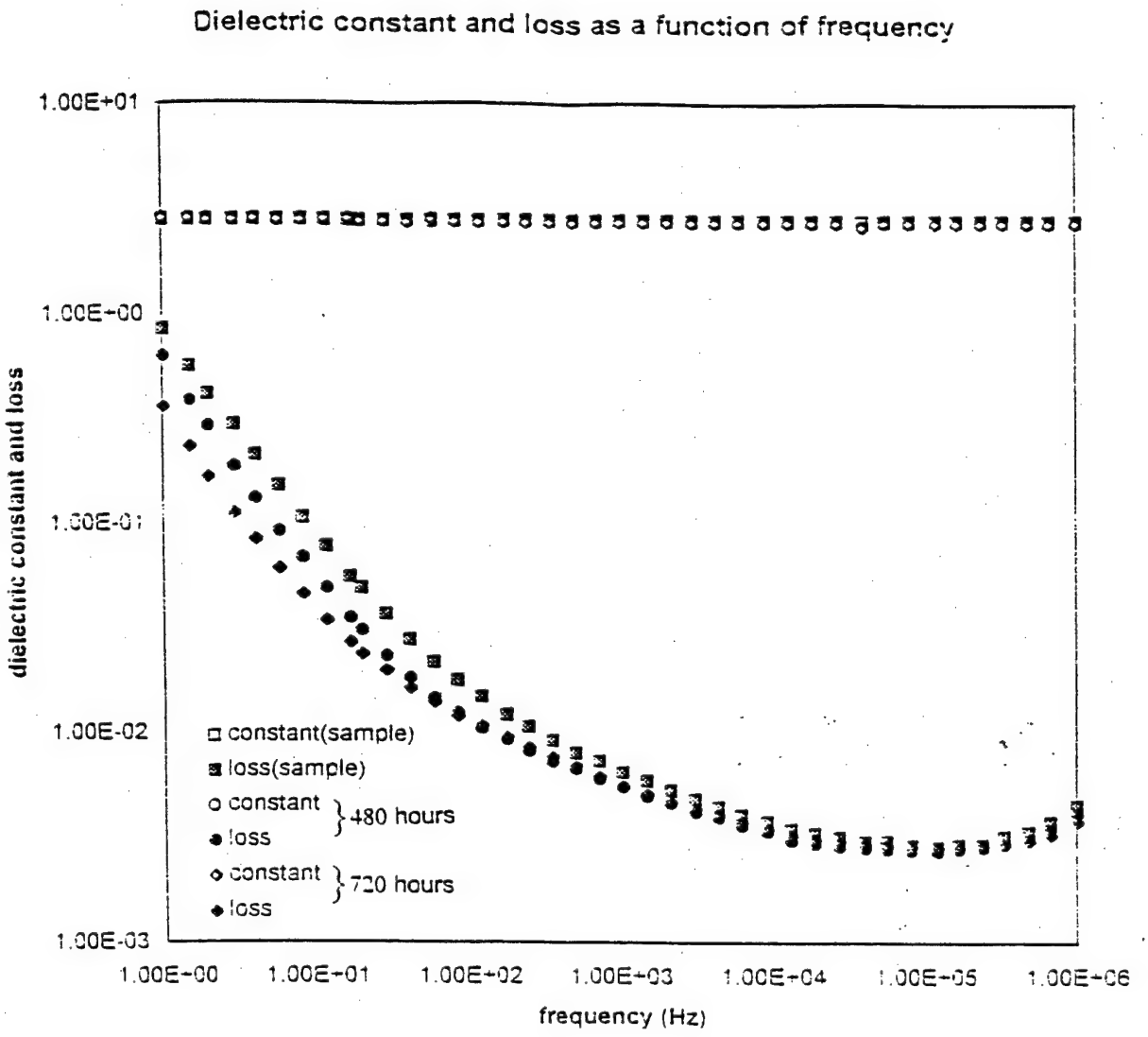

Figure A12. Frequency dependence of the real and the imaginary components of the complex dielectric permittivity of two exposed PAO fluid samples which originated from the recirculating setup and of the non-exposed control.

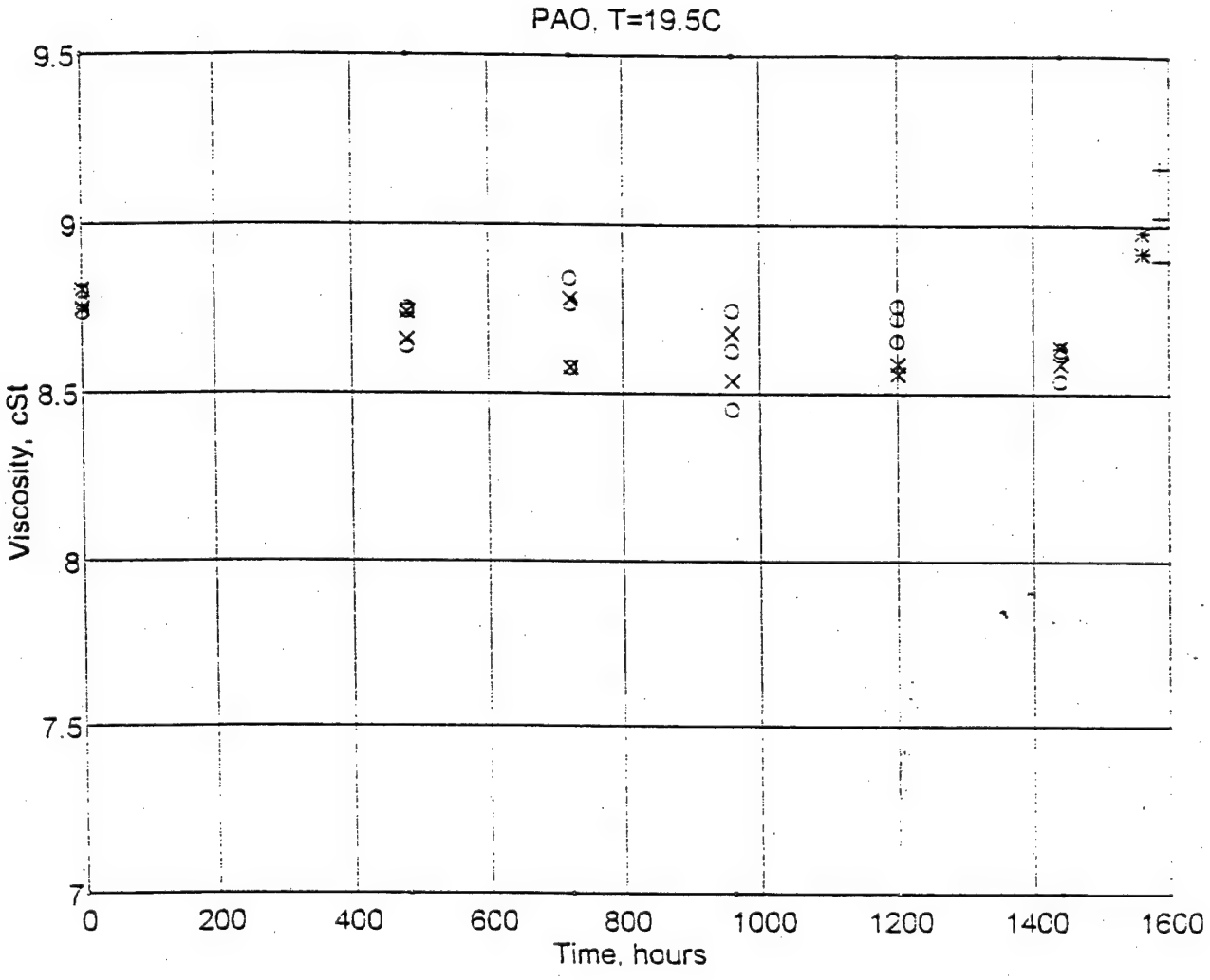

Figure A13. Viscosity of the exposed PAO fluid samples and of (∘) the non-exposed control; ×, samples originated from the recirculating setup and ∗, samples originated from the sparking setup.

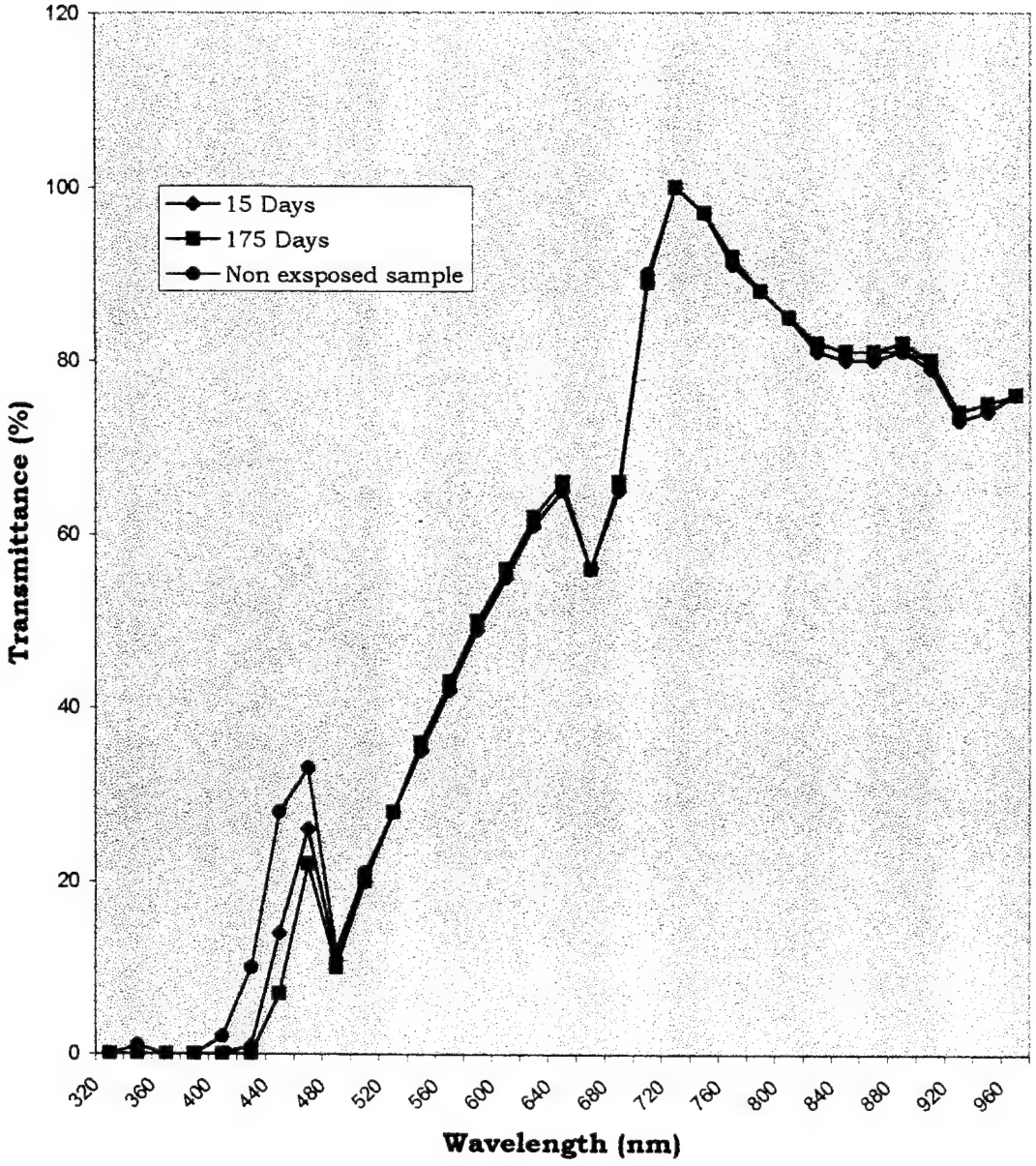

Figure A14a. **Transmittance of the exposed PAO fluid samples originated from the recirculating setup at different times of exposure and of the non-exposed control.**
(the wavelength range from 320 cm^{-1} to 960 cm^{-1}).

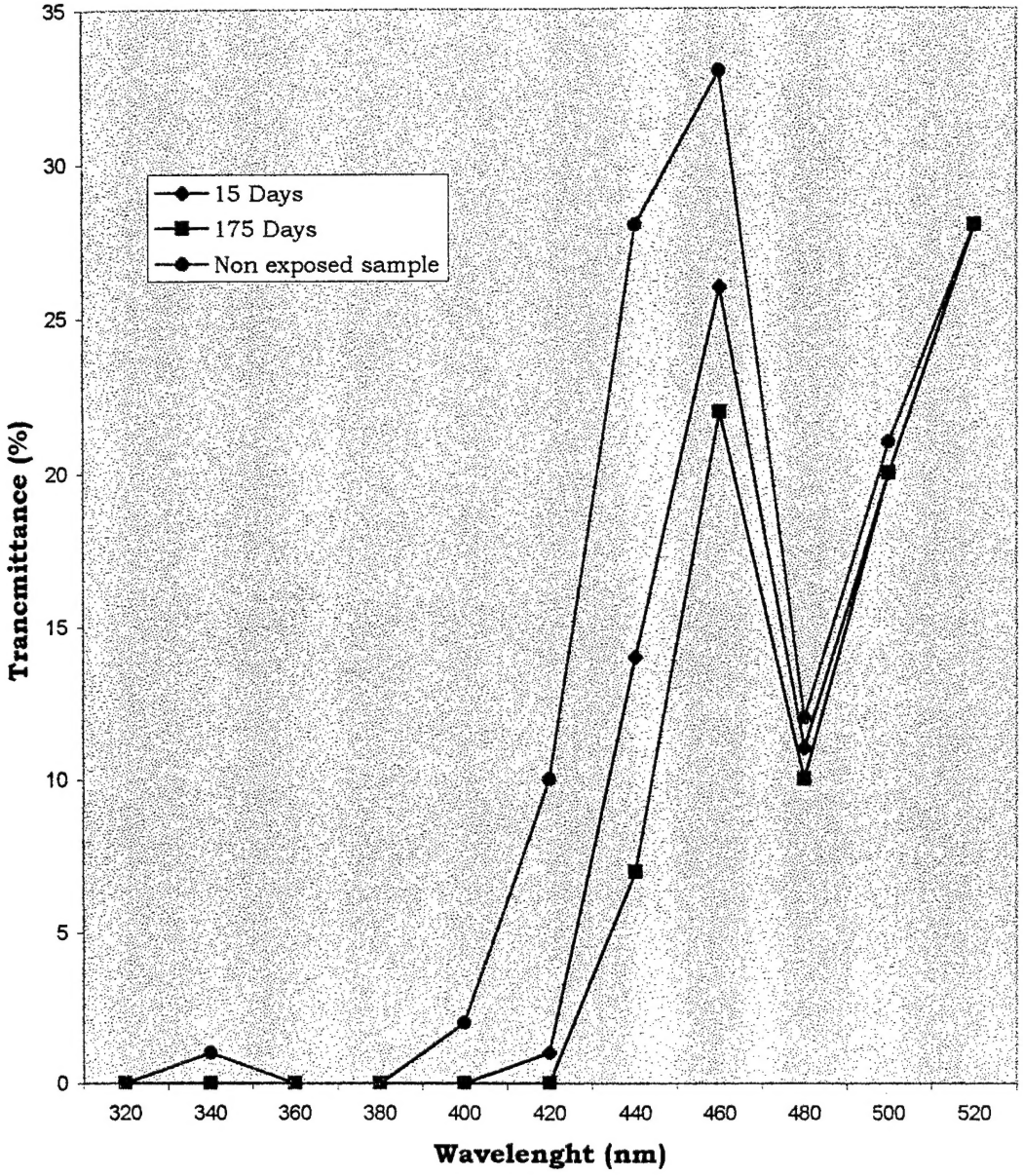

Figure A14b. **Transmittance of the exposed PAO fluid samples originated from the recirculating setup at different times of exposure and of the non-exposed control.**
(enlargement of portion from 320 cm^{-1} to 520 cm^{-1}).

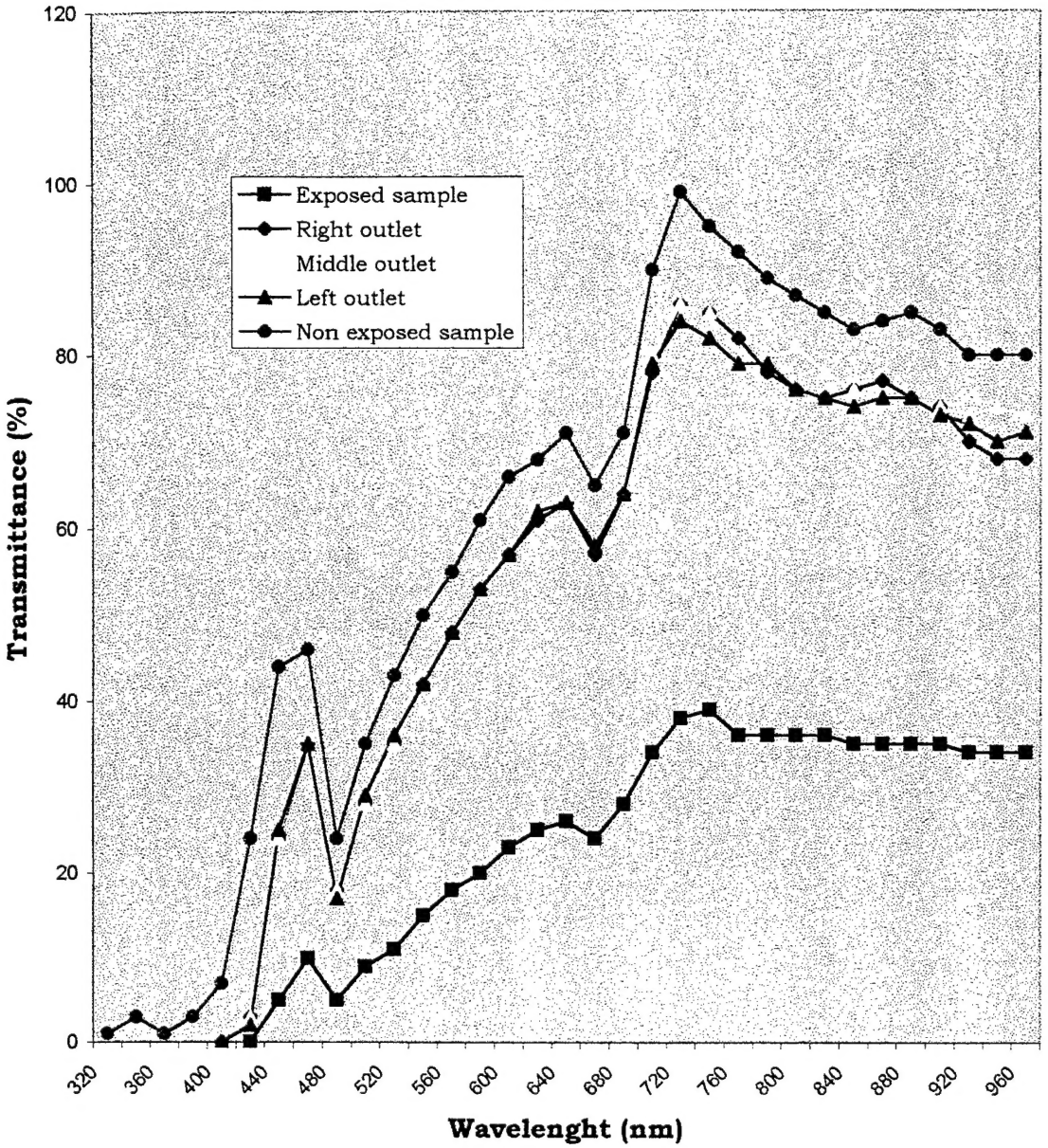

Figure A15. **Transmittance of the exposed PAO fluid sample originated from the sparking setup and of its three fluid portions which came out from the different outlets at the exit of the separator (the flow rate 11ml/min, the applied voltage 3.8kV) as well as of the non-exposed control.**

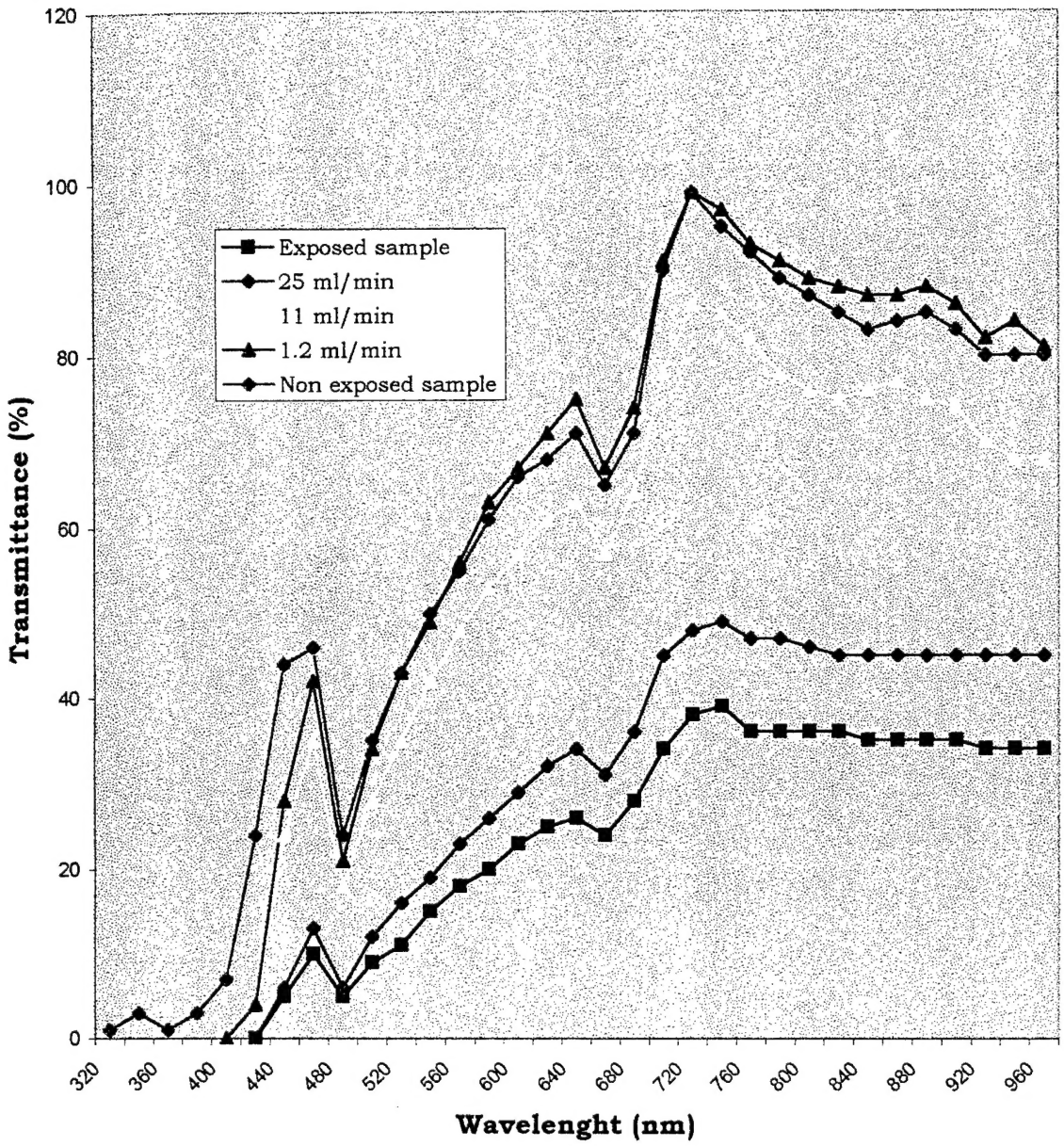

Figure A16. Transmittance of the exposed PAO fluid sample originated from the sparking setup and of its portions coming out of the separator at different flow rates as well of the non-exposed control.

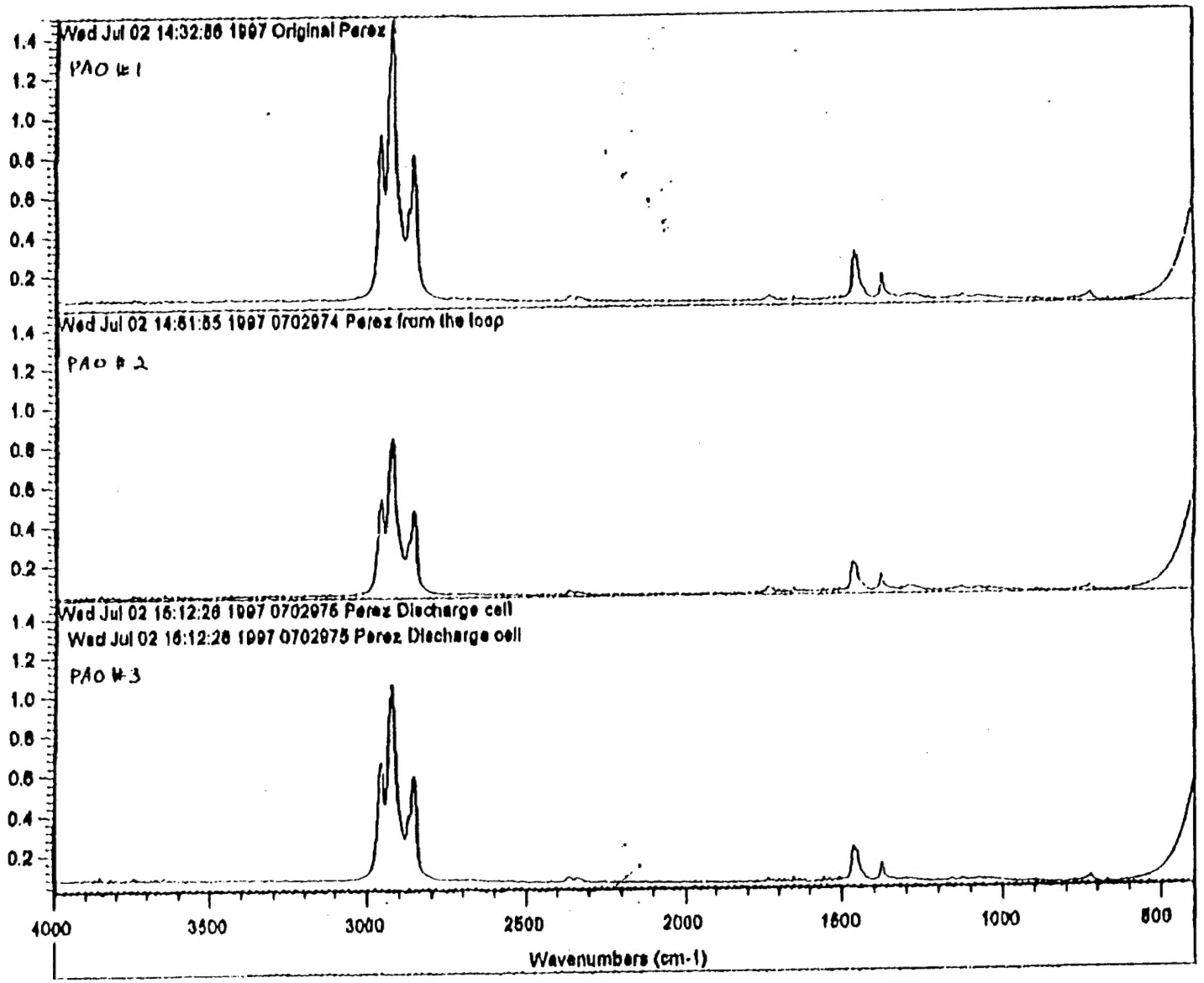

Figure A17. The IR spectra of the exposed PAO fluid samples originated from the recirculating setup and the sparking setup, as well as of the non-exposed control.